

See discussions, stats, and author profiles for this publication at: <https://www.researchgate.net/publication/43347333>

Analysis of Secreted Proteins for the Study of Bladder Cancer Cell Aggressiveness

ARTICLE in JOURNAL OF PROTEOME RESEARCH · JUNE 2010

Impact Factor: 4.25 · DOI: 10.1021/pr100189d · Source: PubMed

CITATIONS

22

READS

18

11 AUTHORS, INCLUDING:



Manousos Makridakis

Biomedical Research Foundation

18 PUBLICATIONS 400 CITATIONS

SEE PROFILE



Maria G Roubelakis

National and Kapodistrian University of At...

37 PUBLICATIONS 676 CITATIONS

SEE PROFILE



Sophia Kossida

Biomedical Research Foundation

139 PUBLICATIONS 843 CITATIONS

SEE PROFILE



Giovanni Candiano

IRCCS Istituto G. Gaslini

189 PUBLICATIONS 3,706 CITATIONS

SEE PROFILE

Analysis of Secreted Proteins for the Study of Bladder Cancer Cell Aggressiveness

Manousos Makridakis,[†] Maria G. Roubelakis,[‡] Vasiliki Bitsika,[‡] Veronica Dimuccio,[§]
Martina Samiotaki,^{||} Sophia Kossida,[†] George Panayotou,^{||} Jonathan Coleman,[⊥]
Giovanni Candiano,[§] Nikolaos P. Anagnou,^{‡, #} and Antonia Vlahou^{*,†}

Biotechnology Division, Biomedical Research Foundation, Academy of Athens, Greece, Laboratory of Cell and Gene Therapy, Biomedical Research Foundation, Academy of Athens, Greece, Laboratory on Physiopathology of Uremia, G. Gaslini Children's Hospital, Genoa, Italy, Institute of Molecular Oncology, Biomedical Sciences Research Center "Alexander Fleming", Vari, Greece, Department of Surgery, Memorial Sloan Kettering Cancer Center, New York, and Laboratory of Biology, University of Athens School of Medicine, Athens Greece

Received March 2, 2010

Secreted proteins play a key role in cell signaling, communication, and migration. We recently described the development of an aggressive variant (T24M) of the bladder cancer cell line T24. Using this cell line model, the objective of our work was the identification of secreted proteins involved in the acquisition of the aggressive phenotype. Using *in vitro* assays, we demonstrate that conditioned media of the T24M cells promote motility of the parental less aggressive T24 cells. Proteomic analysis of cell culture conditioned media by the use of 2-dimensional gel electrophoresis coupled to MALDI TOF MS and LC-MS approaches resulted in enrichment and detection of multiple classical extracellular and secreted proteins such as fibronectin, cystatin, fibrillin, fibulin, interleukin 6, etc. Comparison of the secretome of the T24 and T24M cells indicated differences in proteins with potential involvement in the mechanisms of cell aggressiveness including SPARC, tPA, and clusterin. These findings were further confirmed by Western blot analysis. In the case of SPARC, further studies involving transwell assays indicated that blockage of the protein in the presence of SPARC-specific Abs results in decreased cell motility. Collectively, our study provides a 2DE-based comprehensive analysis of bladder cancer cell secretome. The results indicate various secreted proteins with potential involvement in bladder cancer cell aggressiveness and more specifically provide initial evidence for special role of SPARC in bladder cancer cell motility and invasiveness.

Keywords: bladder cancer • proteomics • T24 • secretome • SPARC • 2DE

Introduction

Bladder cancer is the second in incidence and mortality cancer of the genitourinary system.¹ One of the most important clinical challenges is the identification of the aggressive tumors destined to recur and progress following initial treatment. The prediction rates received by current markers are not optimal, underscoring the need for a continuous search for more reliable prognostic biomarkers. Cell culture and animal models are invaluable research tools utilized to increase our knowledge on the molecular mechanisms of neoplasia, to identify and

characterize diagnostic and prognostic markers, and to pinpoint and evaluate potential drug and therapeutic targets.² We recently reported on the development of an invasive and metastatic bladder cancer cell line model: T24M cells derived from the T24 cells following a series of passages in cell culture and subcutaneous injections in SCID mice.³ Detailed cytogenetic and proteomic characterization of T24M in comparison to their parental cell line showed that these cells exhibit various molecular characteristics frequently encountered in aggressive urothelial carcinomas, constituting thereby a reliable model for the disease.³

Using this metastatic variant, the purpose of this study was the investigation of cell secretome for the identification of proteomic changes that may be associated with the increase of metastatic phenotype. Secreted proteins are well-known to be involved in a variety of important functions associated with cell motility and invasiveness;⁴ nevertheless, their proteomics analysis is quite challenging due to (a) their presence at frequently very low concentrations, (b) their masking and contamination by cytoplasmic or other normally nonsecreted proteins released following cell lysis and death, and (c) masking

* To whom correspondence should be addressed. Antonia Vlahou Ph.D, Biotechnology Division, Biomedical Research Foundation, Academy of Athens, Soranou Efessiou 4, 11527, Athens, Greece. Tel: 30 210 65 97 506. Fax: 30 210 65 97 545. E-mail: vlahoua@bioacademy.gr.

[†] Biotechnology Division, Biomedical Research Foundation, Academy of Athens.

[‡] Laboratory of Cell and Gene Therapy, Biomedical Research Foundation, Academy of Athens.

[§] G. Gaslini Children's Hospital.

^{||} Biomedical Sciences Research Center "Alexander Fleming".

[⊥] Memorial Sloan Kettering Cancer Center.

[#] University of Athens School of Medicine.

by serum proteins (i.e., fetal bovine serum) normally present in the culture media.⁵ Technological advancements in proteomics research have facilitated secretome studies the past few years.^{6–8} As an example, studies have been conducted for the analysis of renal, pancreatic, lung, prostate, breast, and oral carcinomas pointing to various proteins as potential mediators of cell aggressiveness.⁴ In the case of bladder cancer, studies have been conducted using the T24 and RT112 cells in combination to shotgun proteomics^{4,9} as well as by 1D gel analysis and MS on U1 and U4 cell lines.^{4,10} These studies indicated among others the pro-u-plasminogen activator and CXCL1 as proteomics changes putatively associated with increase of aggressive phenotype.^{9,10}

With the current study, we target the analysis of secreted proteins from two lineage related and differing in metastatic potential bladder cancer cell lines: T24 and T24M. The employment of lineage related cells offers the advantage of mimicking the evolution of bladder cancer in a more reliable way in comparison to the employment of unrelated cell lines. 2DE analysis was performed by which various proteomic changes were detected in the T24M compared to the T24 conditioned media (CM) including various proteases as well as proteins involved in tumor-microenvironment interactions such as SPARC, tPA, clusterin, cathepsin L1, and galectin 3 binding protein. Several of these findings were confirmed by immunoblot analysis and in the case of SPARC a preliminary *in vitro* investigation of its function in bladder cell motility was also conducted.

Experimental Procedures

Cell Culture and Sample Preparation for Proteomics Analysis. T24 and T24M cells were grown in DMEM supplemented with 10% FBS (Gibco-Invitrogen, Grand Island, New York) at 37 °C, 5% CO₂ as previously described.³ When the cells reached a concentration of 10⁶ cells per mL, the medium was removed and the cell layer was washed 3 times with 1× PBS (Gibco BRL, Grand Island, NY) and 1 time with Serum and Phenol Red Free Medium (SFM) (Gibco-Invitrogen, Grand Island, New York) SFM was added to the cells for an incubation period of 24 h after which cell layer (described below) as well as SFM were collected. The latter was centrifuged at 1000 g for 10 min at 4 °C to remove dead cells and large debris and incubated with 7.5% TCA (Trichloro Acetic Acid), 0.1% NLS (N-Lauroyl Sarcosine) at –20 °C overnight.⁵ Centrifugation then followed at 10 000× g for 10 min at 4 °C. The supernatant was discarded, and the pellet was washed with ice cold THF (Tetra Hydro Furan) and centrifuged again as previously, and the final pellet was dried in the air and resuspended in Isoelectric Focusing (IEF) sample buffer (7 M urea, 2 M thiourea, 4% CHAPS, 1% DTE, 2% IPG buffer and 3.6% Protease inhibitors) by 30 min bath sonication.⁵ Samples were stored at –20 °C until use.

For the preparation of cell extracts, cells were collected following trypsinization³ and cell pellets were washed 3 times in PBS and dissolved in IEF sample buffer by bath sonication. The suspension was centrifuged at 13 000 rpm for 20 min, supernatants were collected, aliquoted, and stored at –20 °C until usage. Protein concentration was estimated by the use of Bradford reagent (Bio Rad).

Two-Dimensional Electrophoresis (2DE). Conditioned Medium was analyzed by 2DE according to Chevallet et al (2007).⁵ Proteins (500 µg for Coomassie staining-map analysis, or 100 µg for silver-differential expression analysis) were resolved on

17 cm linear strips pH range 4–7 (Bio Rad) using the in gel rehydration method. Second dimensional analysis was performed on 12% SDS-PAGE. The 2DE gels were stained with Silver Quest (Invitrogen) or with Coomassie colloidal blue stain (Novex, Invitrogen) according to the manufacturer's instructions.

Spot Quantification. Gels were scanned at a GS-800 imaging densitometer (Bio Rad) in transmission mode and the images were analyzed using the PD Quest 8 software package (Biorad). Normalization of the individual protein spot quantity was made according to the total quantity of the valid spots in the gel and expressed in ppm. Comparison of the expression level of the various protein spots was conducted by the use of Mann–Whitney and Student's *t*-test. The reported protein spots were found to be differentially expressed ($P < 0.05$, $a = 0.95$).

MALDI-TOF MS (Matrix Assisted Laser Desorption Ionization-Time of Flight Mass Spectrometry). Protein spots were excised manually or automatically by the use of the ProteinerSp Protein picker (Bruker Daltonics). Tryptic digestion and Peptide Mass Fingerprinting (PMF) was performed as previously described.¹¹ In brief, peptide masses were determined by MALDI-TOF/TOF MS (Ultraflex TOF/TOF, Bruker Daltonics, Bremen, Germany), peak list was created with Flexanalysis v2.2 software (Bruker), smoothing was applied with Savitzky-Golay algorithm (width 0.2 *m/z*, cycle number 1), and a Signal/noise threshold ratio of 2.5 was allowed. For peptide matching (Mascot Server 2; Matrix Science), the following settings were used: Monoisotopic mass, one miscleavage site, carbamidomethylation of cysteine as fixed and oxidation of methionine as variable modifications. Stringent criteria were used for protein identification with a maximum allowed mass error of 25 ppm and a minimum of 4 matching peptides. Notably, a large percentage of the proteins were identified based on six matches. The probability of a false identity was usually lower than 10^{–5}. Analysis of the data using a sequence scrambled version of Swiss-Prot generated by the decoy generating- script available at Matrix Science and using the settings described above provided no identifications. All spectra and respective peak lists are provided as Supporting Information (File names: Supplementary Table Annotated Spectra T24CM map PMF 1 and 2, Supplementary Table Annotated Spectra Differential Expression; xls sheet: “Annotated Spectra Differentially Expressed Spots PMF”).

LC–MS/MS (Liquid Chromatography coupled to Mass Spectrometry). In cases where spots could not be identified by PMF, LC–MS/MS analysis was conducted. The protein spots were excised from the gel and cut into small pieces. Following reduction with DTT and alkylation with iodoacetamide, protein in-gel digestion was performed using mass spectrometry grade gold trypsin (Promega, Madison, WI) in 40 mM ammonium carbonate overnight. The resulting peptides were eluted from gel particles with successive washes with 50% acetonitrile and 5% formic acid and then concentrated by SpeedVac to near dryness. The volume of the sample was adjusted to 10 µL with 0.1% formic acid and injected in a nanohigh performance liquid chromatography system (Ultimate, Dionex). Tryptic peptides were separated on a PepMap reversed phase C18 column (75 µm × 15 cm, Dionex). The injected samples were eluted at 180 nL/min with a 2–80% acetonitrile/water gradient containing 0.1% formic acid over 55 min. The separated tryptic fragments were visualized by detection of the absorbance at 214 nm and were introduced online into a LCQ Deca ion-trap mass spectrometer equipped with a nanoelectrospray source (Thermo Fisher Scientific). For the analysis of peptides, data-

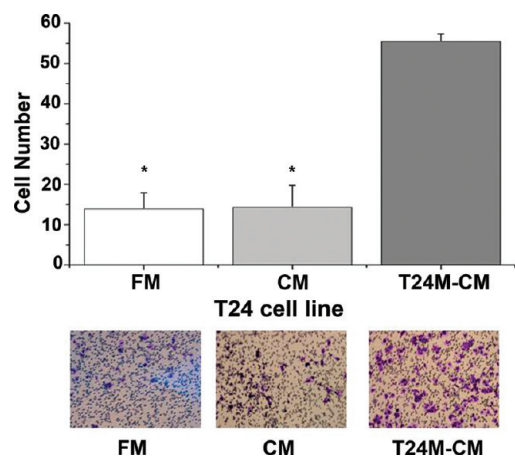


Figure 1. T24M conditioned medium increases migration potential of T24 cells. (Top) Representative diagram of the number of migrated T24 cells toward FM, CM collected from same cells and CM obtained from T24M cells. A significantly greater number of migrated T24 cells toward T24M CM is observed compared to migrated T24 cells toward FM or T24 CM ($p < 0.05$). (Bottom) Optical images of the migrated T24 cells in the presence of FM, CM, and T24M CM. In all cases 50 000 cells were initially plated to the insert of a transwell plate and allowed to migrate for 6 h toward FM or CM, as applicable. The nonmigrated cells were then removed from the top of the insert and migrated cells were fixed and stained (Ral Kit). Migration was quantified by counting the nuclei that passed through the filter from a minimum of 10 fields of view (20 \times) (Leica CTR MIC microscope, Image J software). Three independent experiments were performed including 3 replicates each. Data are presented as the mean \pm SD and were analyzed by Student's *t*-test.

dependent MS/MS experiments were performed. The method consisted of an MS scan (scan event 1) with subsequent MS/MS scans (scan events 2, 3, and 4) of the three most intense ions from the first MS scan. The data were collected using Xcalibur software (Thermo Electron Corp.) and peptide analysis was performed using the TurboSequest algorithm in the BioworksBrowser 3.3 software package (Thermo Electron Corp.) and the human specific IPI v. 3.53 database (EBI). The search was performed using carbamidomethylation of cysteine and oxidation of methionine as variable modifications. Two missed cleavage sites, a peptide mass tolerance of 2.0 amu and fragment ions tolerance of 1.0 amu were allowed. The identified peptides were evaluated using charge state versus cross-correlation number (Xcorr). SEQUEST results were filtered for false-positive identifications. The criteria for positive identification of peptides were Xcorr >1.5 for singly charged ions, Xcorr >2.0 for doubly charged ions, and Xcorr >2.5 for triply charged ions with Delta Correlation Score (DelCn) of 0.1 or higher. In addition, Mascot scores were calculated by analyzing raw data with Mascot Distiller software (version 2.3.2.0) using the following settings for the search: carbamidomethylation of cysteine as fixed modification, oxidation of methionine, histidine, tryptophan and deamidation of asparagine and glutamine as variable modifications. One missed cleavage site, a peptide mass tolerance of 2.5 Da, and a fragment mass tolerance of 0.7 Da were allowed. MS/MS spectra and fragmentation tables, in the case of one peptide identifications, as well as detailed information on all identification parameters are provided as Supporting Information (Filename: Supplementary Table Annotated Spectra Differential Expression; xls sheets: "MS-MS

spectra 1peptide ID" and "Differentially Expressed spots LC-MS-MS", respectively).

Western Blot Analysis. Total proteins (10 μ g) of T24 CM and T24M CM were separated by 10% SDS-PAGE under reducing conditions and electroblotted to Hybond-ECL nitrocellulose membrane (Amersham Biosciences). After blocking with 5% nonfat dried milk in TBST (20 mM Tris/pH 7.6, 137 mM NaCl, 0.1% Tween 20) for 2 h at room temperature, membranes were washed with TBST and incubated overnight at 4 $^{\circ}$ C with the primary antibodies, as applicable: mouse antihuman SPARC (Santa Cruz; dilution 1:500), mouse antihuman tPA (Santa Cruz; dilution 1:500), goat antihuman clusterin (Santa Cruz; dilution 1:1000). Membranes were then washed with TBST and incubated with antimouse or antigoat HRP-conjugated secondary antibody (Santa Cruz; dilution 1:10 000) for 2 h at room temperature. A final wash with TBST was made and target protein was detected by Enhanced Chemiluminescence (Perkin-Elmer LAS, Inc.) detection system. Films were scanned and images were analyzed using Quantity One software (Bio Rad).

Transwell Migration Assay-In Vitro Blocking Experiments. *In vitro* motility assays were performed as previously described.³ In brief, T24 or T24M cells were cultured for 48 h in DMEM supplemented with 2% FBS and then were transferred, at $5 \times 10^4/100 \mu$ L density, to the insert of a transwell plate with 5 μ m pore size (Corning-Costar, Cambridge, MA). The cells were then allowed to migrate for 6 h across the pore membrane, toward DMEM supplemented with 2% FBS fresh medium (FM), or CM. After the 6 h incubation period, the nonmigrated cells were removed from the top of the insert with a wet cotton swab. The migrated cells were then fixed with 4% paraformaldehyde (Sigma-Aldrich) on the membrane and stained using the Ral Kit (Ral Reactif, Paris, France) according to the manufacturer's instructions. Migration was quantified by counting the nuclei that passed through the filter. Photographs from the stained nuclei were taken from a minimum of 10 fields of view (20 \times) for each membrane using a Leica CTR MIC microscope and then were counted by using Image J software. Three independent experiments were performed including 3 replicates each. Statistical analysis was performed using Student's *t*-test.

For the *in vitro* blocking experiments, SPARC was blocked in T24M CM and T24M cells by incubating CM and cells, as applicable, with a monoclonal antibody of SPARC (Santa Cruz) at a dilution of 1:100 and 1:10 respectively, for 30 min at 4 $^{\circ}$ C. Cells and CM were also incubated at the same conditions with isotype IgG1 control Ab (Becton Dickinson). After this incubation period, *in vitro* motility assays were performed for T24M cells as described above. Migration percentage was normalized to the migration of the nontreated cells to nontreated CM, which was set to 100%.

Immunohistochemistry with SPARC Antibody. NOD-SCID immunodeficient mice were bred and maintained at BRFAA, (Athens, Greece) under approved animal care protocols. Mice ($n = 6$) were used in accordance with institutional guidelines under approved protocols. One million T24M cells were administered subcutaneously, as suspension in 200 μ L of PBS, into the tail base of the animals.³ Tumors were excised one month after the T24M injection, fixed in 4% neutral buffered formalin (Sigma-Aldrich) and five micrometer thick paraffin sections were prepared. Tissue sections were dewaxed in xylene and then rehydrated in graded alcohol. Endogenous peroxidase activity was blocked with 0.3% hydrogen peroxide in methanol. Nonspecific binding was blocked using 10% donkey serum in PBS. Sections were subsequently incubated with anti-SPARC

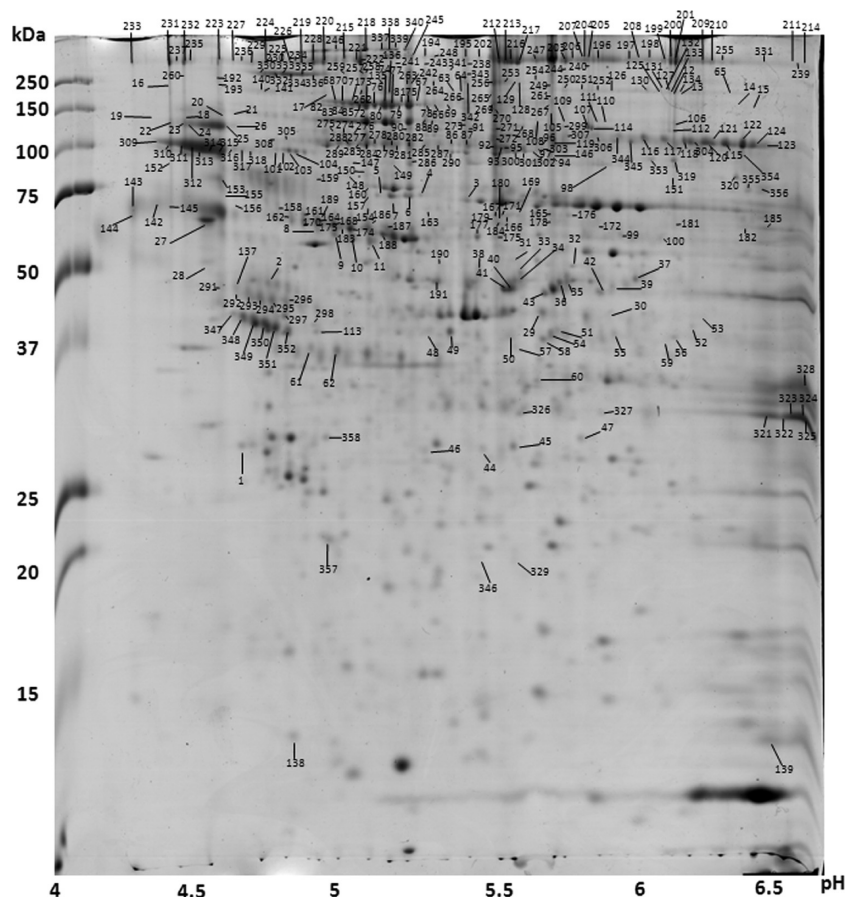


Figure 2. Representative 2DE gel from T24 conditioned medium. Five hundred micrograms of T24 CM were applied on 17 cm linear strips pH range 4–7 (Biorad) using the in gel rehydration method. Spot detection was performed by Coomassie colloidal blue. Six hundred and ninety four protein spots were identified (provided in Supplementary Table T24CM map and Supplementary Figure 1) using PMF analysis. Three hundred and fifty eight protein spots (51%) were found as secreted (according to GO; definition of “secreted” is provided in Table 1-legend) corresponding to 46 different gene products (Table 1). The location of these proteins in the gel is depicted. Numbers correspond to spot numbers of Table 1.

antibody (Santa Cruz dilution 1:50) or appropriate isotype control (Becton Dickinson). The reaction was developed with biotinylated goat antimouse secondary antibody (DakoCytomation), followed by ABC-complex-HRP (DakoCytomation) and DAB (Vector Laboratories). Finally, the slides were counterstained in Gill's hematoxylin (Sigma-Aldrich). The cells were visualized and photographed on a Leica CTR-MIC microscope.

Results

T24M CM Increases Motility of T24 Cells In Vitro. The migration potential of T24 and T24M cells toward CM was investigated by *in vitro* migration assays. In order to enhance the signal of secreted molecules and facilitate the study of their effects, low serum concentration (2%FBS) was used. T24M cells have been previously shown³ to exhibit increased migration potential to their CM compared to T24 cells. Moreover, T24M cells migrated faster to their CM compared to FM, indicating that they might secrete factors or molecules that promote cell motility. In support of this hypothesis the effect of T24M CM in T24 cells motility was investigated. As shown (Figure 1), the migration ability of T24 cells was significantly increased toward T24M CM. On the other hand T24M cells motility did not seem to be affected by T24 CM (data not shown). Collectively, these results suggest that T24M cells exhibit enhanced motility properties which may be related to factors that they produce and secrete.

Protein Map of T24 Conditioned Medium. To investigate the secretome of the two cell lines, their conditioned media were analyzed by 2DE in 4–7 linear pH gradient strips. Special care was given to decrease as possible contamination by cellular proteins and serum albumin, as described in materials and methods. In addition, to demonstrate specificity of findings, respective cell extracts were in parallel analyzed (Figure 3).

The derived pattern of resolved protein spots for each cell type was highly consistent. Representative 2DE gel from T24 conditioned medium is shown in Figure 2. Six hundred and ninety four proteins were identified (Supplementary Table-T24 CM Map). Of these, 358 protein spots (51%) were found as secreted (according to GO-definition of “secreted” is provided in Table 1 legend) corresponding to 46 different gene products (Table 1). The location of these proteins in the gel is depicted (Figure 2). As expected, an over-representation of ECM structural proteins (such as collagens, fibronectin, laminins, fibrillin, fibulin), proteases and protease inhibitors (MMP2, cathepsins, members of complement, cystatins), matricellular proteins (SPARC, galectin 3 binding protein) and isoforms thereof was observed. Additionally, proteins with growth factor activity and/or pronounced roles in signal transduction, frequently encountered at low concentrations were also detected such as interleukin 6, insulin-like growth factor-binding protein 4, stem cell growth factor (eg C-type lectin domain family 11 member A),

Table 1. Secreted Proteins Identified in T24 Conditioned Medium^a

spot number	protein	accession name	Mascot score	peptides matched	peptides unmatched	sequence coverage %	theoretical MW Da	theoretical pI-value	experimental MW Da	experimental pI-value	comments
1	14-3-3 protein sigma	143S_HUMAN	96	29	42	52	27871	4.5	28000	4.6	modulation of kinase activity/growth factor
2	45 kDa calcium-binding protein precursor	CAB45_HUMAN	92	13	34	37	41895	4.6	49000	4.8	exocytosis
3	72 kDa type IV collagenase precursor	MMP2_HUMAN	78	11	24	19	74918	5.1	74000	5.4	protease/collagen degradation
4	72 kDa type IV collagenase precursor	MMP2_HUMAN	254	28	30	46	74918	5.1	74000	5.2	
5	72 kDa type IV collagenase precursor	MMP2_HUMAN	212	24	28	41	74918	5.1	74000	5.1	
6	72 kDa type IV collagenase precursor	MMP2_HUMAN	244	32	46	50	74918	5.1	74000	5.2	
7	72 kDa type IV collagenase precursor	MMP2_HUMAN	240	34	54	52	74918	5.1	74000	5.2	
8	alpha-1-antitrypsin precursor	AIAT_HUMAN	151	17	48	42	46878	5.3	60000	4.9	protease inhibitor
9	alpha-1-antitrypsin precursor	AIAT_HUMAN	144	16	44	42	46878	5.3	58000	5	
10	alpha-1-antitrypsin precursor	AIAT_HUMAN	116	13	37	32	46878	5.3	57000	5	
11	alpha-1-antitrypsin precursor	AIAT_HUMAN	116	13	40	35	46878	5.3	56000	5.1	
12	alpha-2-macroglobulin precursor	A2MG_HUMAN	75	9	21	7	164600	6	160000	6.1	protease inhibitor/cytokine binding
13	alpha-2-macroglobulin precursor	A2MG_HUMAN	67	16	40	14	164600	6	160000	6.2	
14	alpha-2-macroglobulin precursor	A2MG_HUMAN	79	16	30	14	164600	6	150000	6.4	
15	alpha-2-macroglobulin precursor	A2MG_HUMAN	69	8	23	8	164600	6	149000	6.4	
16	alpha-2-macroglobulin precursor	A2MG_HUMAN	59	8	30	7	164600	6	240000	4.4	
17	alpha-2-macroglobulin precursor	A2MG_HUMAN	61	9	33	7	164600	6	160000	4.9	
18	amyloid beta A4 protein precursor	A4_HUMAN	73	16	47	20	87914	4.4	140000	4.4	protease inhibitor/Notch signaling
19	amyloid beta A4 protein precursor	A4_HUMAN	86	10	22	13	87914	4.6	140000	4.4	
20	amyloid beta A4 protein precursor	A4_HUMAN	90	17	31	20	87914	4.6	140000	4.6	protease inhibitor/Notch signaling
21	amyloid beta A4 protein precursor	A4_HUMAN	87	18	41	21	87914	4.6	140000	4.6	
22	amyloid beta A4 protein precursor	A4_HUMAN	118	20	41	26	87914	4.6	140000	4.4	
23	amyloid beta A4 protein precursor	A4_HUMAN	134	24	37	27	87914	4.6	140000	4.4	
24	amyloid beta A4 protein precursor	A4_HUMAN	168	30	36	30	87914	4.6	140000	4.5	
25	amyloid beta A4 protein precursor	A4_HUMAN	256	40	50	38	87914	4.6	140000	4.6	
26	amyloid beta A4 protein precursor	A4_HUMAN	97	15	22	18	87914	4.6	140000	4.6	
27	calreticulin precursor	CALR_HUMAN	225	23	58	55	48283	4.1	60000	4.5	steroid hormone receptor regulation/integrin binding
28	calumenin precursor	CALU_HUMAN	68	7	19	27	37198	4.3	50000	4.5	Calcium binding
29	cathepsin B precursor	CATB_HUMAN	121	15	33	40	38766	5.9	40000	5.7	protease
30	cathepsin B precursor	CATB_HUMAN	102	11	28	38	38766	5.9	40000	5.9	
31	cathepsin D precursor	CATD_HUMAN	126	16	24	39	45037	6.1	50000	5.6	
32	cathepsin D precursor	CATD_HUMAN	149	22	45	49	45037	6.1	49000	5.8	protease
33	cathepsin D precursor	CATD_HUMAN	128	19	41	46	45037	6.1	49000	5.6	
34	cathepsin D precursor	CATD_HUMAN	143	23	50	47	45037	6.1	48000	5.6	
35	cathepsin D precursor	CATD_HUMAN	132	18	29	44	45037	6.1	47000	5.8	
36	cathepsin D precursor	CATD_HUMAN	153	22	42	47	45037	6.1	47000	5.8	
37	cathepsin D precursor	CATD_HUMAN	114	15	24	39	45037	6.1	48000	6	
38	cathepsin D precursor	CATD_HUMAN	120	17	36	41	45037	6.1	49000	5.5	
39	cathepsin D precursor	CATD_HUMAN	67	11	46	30	45037	6.1	47000	5.9	
40	cathepsin D precursor	CATD_HUMAN	160	24	47	51	45037	6.1	47000	5.6	
41	cathepsin D precursor	CATD_HUMAN	209	22	20	48	45037	6.1	47000	5.6	
42	cathepsin D precursor	CATD_HUMAN	117	14	21	35	45037	6.1	47000	5.9	
43	cathepsin D precursor	CATD_HUMAN	142	23	50	51	45037	6.1	46000	5.7	
44	cathepsin D precursor	CATD_HUMAN	68	12	31	27	45037	6.1	27000	5.5	
45	cathepsin D precursor	CATD_HUMAN	81	13	31	32	45037	6.1	27000	5.6	
46	cathepsin D precursor	CATD_HUMAN	102	14	23	33	45037	6.1	27000	5.3	
47	cathepsin D precursor	CATD_HUMAN	71	9	25	19	45037	6.1	27000	5.8	protease
48	cathepsin L1 precursor	CATL1_HUMAN	100	14	23	33	37996	5.2	37000	5.3	protease
49	cathepsin L1 precursor	CATL1_HUMAN	93	18	52	41	37996	5.2	37000	5.4	protease
50	cathepsin Z precursor	CATZ_HUMAN	51	4	19	16	34530	6.9	37000	5.6	
51	cathepsin Z precursor	CATZ_HUMAN	114	12	36	44	34530	6.9	37000	5.7	
52	cathepsin Z precursor	CATZ_HUMAN	105	11	30	44	34530	6.9	37000	6.2	
53	cathepsin Z precursor	CATZ_HUMAN	60	7	38	29	34530	6.9	38000	6.2	
54	cathepsin Z precursor	CATZ_HUMAN	114	14	36	44	34530	6.9	37000	5.7	
55	cathepsin Z precursor	CATZ_HUMAN	60	6	22	27	34530	6.9	37000	5.9	
56	cathepsin Z precursor	CATZ_HUMAN	123	13	28	44	34530	6.9	37000	6.2	

Table 1. Continued

spot number	protein	accession name	Mascot score	peptides matched	peptides unmatched	sequence coverage %	theoretical MW Da	theoretical pI-value	experimental MW Da	experimental pI-value	comments
57	cathepsin Z precursor	CATZ_HUMAN	66	9	46	34	34530	6.9	37000	5.6	
58	cathepsin Z precursor	CATZ_HUMAN	102	14	36	41	34530	6.9	37000	5.7	
59	cathepsin Z precursor	CATZ_HUMAN	76	9	34	34	34530	6.9	37000	6.1	
60	cathepsin Z precursor	CATZ_HUMAN	70	6	38	27	34530	6.9	35000	5.7	
61	clusterin precursor	CLUS_HUMAN	59	5	24	16	53031	5.9	37000	4.9	signal trasduction/complement activation
62	clusterin precursor	CLUS_HUMAN	51	4	19	14	53031	5.9	37000	5	ECM structure
63	collagen alpha-1(VI) chain precursor	CO6A1_HUMAN	64	9	43	11	109602	5.1	150000	5.4	
64	collagen alpha-1(VI) chain precursor	CO6A1_HUMAN	78	11	49	13	109602	5.1	150000	5.4	
65	collagen alpha-1(VI) chain precursor	CO6A1_HUMAN	64	8	32	10	109602	5.1	150000	6.3	
66	collagen alpha-1(VI) chain precursor	CO6A1_HUMAN	90	18	45	21	109602	5.1	150000	5.3	
67	collagen alpha-1(VI) chain precursor	CO6A1_HUMAN	84	14	35	19	109602	5.1	150000	5.3	
68	collagen alpha-1(VI) chain precursor	CO6A1_HUMAN	121	21	38	23	109602	5.1	150000	5	
69	collagen alpha-1(VI) chain precursor	CO6A1_HUMAN	67	14	43	17	109602	5.1	150000	5.4	
70	collagen alpha-1(VI) chain precursor	CO6A1_HUMAN	123	24	57	28	109602	5.1	150000	5	
71	collagen alpha-1(VI) chain precursor	CO6A1_HUMAN	127	24	56	30	109602	5.1	150000	5	
72	collagen alpha-1(VI) chain precursor	CO6A1_HUMAN	146	27	55	29	109602	5.1	150000	5	
73	collagen alpha-1(VI) chain precursor	CO6A1_HUMAN	128	26	63	27	109602	5.1	150000	5.1	
74	collagen alpha-1(VI) chain precursor	CO6A1_HUMAN	178	31	59	34	109602	5.1	150000	5.1	
75	collagen alpha-1(VI) chain precursor	CO6A1_HUMAN	147	27	61	32	109602	5.1	150000	5.2	
76	collagen alpha-1(VI) chain precursor	CO6A1_HUMAN	133	26	61	31	109602	5.1	150000	5.1	
77	collagen alpha-1(VI) chain precursor	CO6A1_HUMAN	133	26	61	31	109602	5.1	150000	5.2	ECM structure
78	collagen alpha-1(VI) chain precursor	CO6A1_HUMAN	97	19	47	24	109602	5.1	150000	5.3	
79	collagen alpha-1(VI) chain precursor	CO6A1_HUMAN	166	29	55	32	109602	5.1	150000	5.2	
80	collagen alpha-1(VI) chain precursor	CO6A1_HUMAN	162	27	48	31	109602	5.1	150000	5.1	
81	collagen alpha-1(VI) chain precursor	CO6A1_HUMAN	170	26	40	29	109602	5.1	150000	5.2	
82	collagen alpha-1(VI) chain precursor	CO6A1_HUMAN	80	11	17	12	109602	5.1	150000	4.9	
83	collagen alpha-1(VI) chain precursor	CO6A1_HUMAN	145	19	26	24	109602	5.1	150000	4.9	
84	collagen alpha-1(VI) chain precursor	CO6A1_HUMAN	145	23	36	26	109602	5.1	150000	5	
85	collagen alpha-1(VI) chain precursor	CO6A1_HUMAN	130	22	39	26	109602	5.1	150000	5	
86	complement C1r subcomponent precursor	C1R_HUMAN	183	23	44	45	81661	5.9	100000	5.4	protease-immune response
87	complement C1r subcomponent precursor	C1R_HUMAN	192	27	59	47	81661	5.9	100000	5.4	
88	complement C1r subcomponent precursor	C1R_HUMAN	89	15	63	29	81661	5.9	105000	5.3	
89	complement C1r subcomponent precursor	C1R_HUMAN	115	15	38	29	81661	5.9	105000	5.3	
90	complement C1r subcomponent precursor	C1R_HUMAN	66	9	68	17	81661	5.9	104000	5.2	
91	complement C1r subcomponent precursor	C1R_HUMAN	135	13	12	24	81661	5.9	104000	5.4	
92	complement C1r subcomponent precursor	C1R_HUMAN	230	30	57	52	81661	5.9	100000	5.5	
93	complement C1r subcomponent precursor	C1R_HUMAN	189	26	53	47	81661	5.9	100000	5.5	
94	complement C1r subcomponent precursor	C1R_HUMAN	70	9	22	17	81661	5.9	90000	5.7	protease-immune response
95	complement C1s subcomponent precursor	C1S_HUMAN	136	22	61	38	81661	5.9	100000	5.6	
96	complement C1s subcomponent precursor	C1S_HUMAN	177	23	40	43	81661	5.9	100000	5.7	
97	complement C1s subcomponent precursor	C1S_HUMAN	109	13	27	27	81661	5.9	100000	5.7	
98	complement C1s subcomponent precursor	C1S_HUMAN	138	15	22	30	81661	5.9	80000	5.9	
99	complement C1s subcomponent precursor	C1S_HUMAN	61	8	24	17	81661	5.9	60000	6	
100	complement C1s subcomponent precursor	C1S_HUMAN	69	11	36	23	81661	5.9	58000	6.1	
101	complement C1s subcomponent precursor	C1S_HUMAN	67	11	38	22	78174	4.7	90000	4.8	
102	complement C1s subcomponent precursor	C1S_HUMAN	238	32	54	45	78174	4.7	90000	4.8	
103	complement C1s subcomponent precursor	C1S_HUMAN	255	34	51	45	78174	4.7	90000	4.8	
104	complement C1s subcomponent precursor	C1S_HUMAN	163	21	34	34	78174	4.7	90000	4.8	
105	complement C3 precursor	CO3_HUMAN	82	15	57	11	188569	6	140000	5.7	peptidase inhibitor
106	complement C3 precursor	CO3_HUMAN	63	10	37	7	188569	6	130000	6.2	
107	complement C3 precursor	CO3_HUMAN	241	44	39	28	188569	6	130000	5.8	
108	complement C3 precursor	CO3_HUMAN	85	13	33	9	188569	6	130000	5.7	
109	complement C3 precursor	CO3_HUMAN	117	23	34	16	188569	6	130000	5.8	
110	complement C3 precursor	CO3_HUMAN	139	28	33	19	188569	6	130000	5.9	
111	complement C3 precursor	CO3_HUMAN	125	23	25	17	188569	6	130000	5.9	
112	complement C3 precursor	CO3_HUMAN	94	12	26	9	188569	6	125000	6.1	
113	complement C3 precursor	CO3_HUMAN	60	11	28	6	188569	6	37000	4.9	

Table 1. Continued

spot number	protein	accession name	Mascot score	peptides matched	peptides unmatched	sequence coverage %	theoretical MW Da	theoretical pI-value	experimental MW Da	experimental pI-value	comments
114	complement C3 precursor	CO3_HUMAN	246	36	20	24	188569	6	130000	5.9	
115	complement factor B precursor	CFAB_HUMAN	63	7	39	14	86847	6.7	100000	6.3	protease-immune response
116	complement factor B precursor	CFAB_HUMAN	139	20	48	33	86847	6.7	100000	6	
117	complement factor B precursor	CFAB_HUMAN	220	27	39	38	86847	6.7	100000	6.1	protease-immune response
118	complement factor B precursor	CFAB_HUMAN	114	17	48	29	86847	6.7	100000	6.2	
119	complement factor B precursor	CFAB_HUMAN	61	11	51	21	86847	6.7	10000	5.7	
120	complement factor B precursor	CFAB_HUMAN	209	27	47	39	86847	6.7	100000	6.3	
121	complement factor B precursor	CFAB_HUMAN	119	17	41	29	86847	6.7	100000	6.3	
122	complement factor B precursor	CFAB_HUMAN	205	28	54	37	86847	6.7	100000	6.4	
123	complement factor B precursor	CFAB_HUMAN	198	28	58	39	86847	6.7	100000	6.5	
124	complement factor B precursor	CFAB_HUMAN	151	20	39	31	86847	6.7	100000	6.4	
125	complement factor H precursor	CFAH_HUMAN	255	35	30	32	143680	6.2	200000	6.1	immune response
126	complement factor H precursor	CFAH_HUMAN	230	34	35	30	143680	6.2	200000	5.9	
127	complement factor H precursor	CFAH_HUMAN	216	35	45	30	143680	6.2	200000	6.1	
128	complement factor H precursor	CFAH_HUMAN	164	25	30	23	143680	6.2	200000	5.6	
129	complement factor H precursor	CFAH_HUMAN	151	22	24	21	143680	6.2	200000	5.6	
130	complement factor H precursor	CFAH_HUMAN	218	32	33	29	143680	6.2	200000	6	
131	complement factor H precursor	CFAH_HUMAN	288	36	23	32	143680	6.2	200000	6.1	
132	complement factor H precursor	CFAH_HUMAN	161	24	27	26	143680	6.2	200000	6.1	
133	complement factor H precursor	CFAH_HUMAN	212	30	27	26	143680	6.2	200000	6.1	
134	complement factor H precursor	CFAH_HUMAN	225	32	30	29	143680	6.2	200000	6.2	
135	complement factor H precursor	CFAH_HUMAN	90	22	61	29	143680	6.2	200000	5.1	
136	complement factor H precursor	CFAH_HUMAN	145	28	55	27	143680	6.2	190000	5.1	
137	C-type lectin domain family 11 member A precursor	CLC11_HUMAN	63	7	29	19	36015	4.9	47000	4.6	growth factor
138	cystatin-S precursor	CYTS_HUMAN	62	4	32	45	16489	4.8	14000	4.8	protease inhibitor
139	cystatin-SN precursor	CYTN_HUMAN	59	4	39	45	16579	7.7	13000	6.5	protease inhibitor
140	cysteine-rich motor neuron 1 protein precursor	CRIM1_HUMAN	85	9	21	10	121073	5	200000	4.7	BMP activity modulator
141	cysteine-rich motor neuron 1 protein precursor	CRIM1_HUMAN	72	11	26	16	121073	5	200000	4.7	
142	diclkopf-related protein 3 precursor	DKK3_HUMAN	73	8	21	27	39463	4.4	70000	4.4	
143	diclkopf-related protein 3 precursor	DKK3_HUMAN	105	13	25	37	39463	4.4	70000	4.3	
144	diclkopf-related protein 3 precursor	DKK3_HUMAN	74	11	35	34	39463	4.4	70000	4.3	
145	diclkopf-related protein 3 precursor	DKK3_HUMAN	58	6	23	26	39463	4.4	70000	4.4	wnt signaling
146	EGF-containing fibulin-like extracellular matrix protein 1 precursor	FBLN3_HUMAN	66	9	27	19	56885	4.8	90000	5.7	ECM structure
147	EGF-containing fibulin-like extracellular matrix protein 1 precursor	FBLN3_HUMAN	118	15	43	38	56885	4.8	85000	5	
148	EGF-containing fibulin-like extracellular matrix protein 1 precursor	FBLN3_HUMAN	86	12	40	31	56885	4.8	80000	5	
149	EGF-containing fibulin-like extracellular matrix protein 1 precursor	FBLN3_HUMAN	109	14	27	27	56885	4.8	85000	5.2	
150	EGF-containing fibulin-like extracellular matrix protein 1 precursor	FBLN3_HUMAN	98	12	30	29	56885	4.8	82000	5.1	
151	EGF-containing fibulin-like extracellular matrix protein 1 precursor	FBLN3_HUMAN	66	5	11	12	56885	4.8	80000	6.1	
152	EGF-containing fibulin-like extracellular matrix protein 1 precursor	FBLN3_HUMAN	56	6	19	12	56885	4.8	85000	4.4	
153	EGF-containing fibulin-like extracellular matrix protein 1 precursor	FBLN3_HUMAN	148	22	64	50	56885	4.8	80000	4.6	
154	EGF-containing fibulin-like extracellular matrix protein 1 precursor	FBLN3_HUMAN	79	11	39	27	56885	4.8	65000	5.1	
155	EGF-containing fibulin-like extracellular matrix protein 1 precursor	FBLN3_HUMAN	172	21	53	48	56885	4.8	75000	4.6	
156	EGF-containing fibulin-like extracellular matrix protein 1 precursor	FBLN3_HUMAN	170	19	31	41	56885	4.8	70000	4.6	ECM structure
157	EGF-containing fibulin-like extracellular matrix protein 1 precursor	FBLN3_HUMAN	91	13	46	32	56885	4.8	75000	5.1	

Table 1. Continued

spot number	protein	accession name	Mascot score	peptides matched	peptides unmatched	sequence coverage %	theoretical MW Da	theoretical pI-value	experimental MW Da	experimental pI-value	comments
158	EGF-containing fibulin-like extracellular matrix protein 1 precursor	FBLN3_HUMAN	173	20	36	42	56885	4.8	70000	4.8	
159	EGF-containing fibulin-like extracellular matrix protein 1 precursor	FBLN3_HUMAN	103	12	26	26	56885	4.8	80000	4.9	
160	EGF-containing fibulin-like extracellular matrix protein 1 precursor	FBLN3_HUMAN	72	11	41	23	56885	4.8	75000	5.1	
161	EGF-containing fibulin-like extracellular matrix protein 1 precursor	FBLN3_HUMAN	233	29	54	56	56885	4.8	68000	4.8	
162	EGF-containing fibulin-like extracellular matrix protein 1 precursor	FBLN3_HUMAN	131	16	41	40	56885	4.8	66000	4.8	
163	EGF-containing fibulin-like extracellular matrix protein 1 precursor	FBLN3_HUMAN	61	7	31	15	56885	4.8	69000	5.3	
164	EGF-containing fibulin-like extracellular matrix protein 1 precursor	FBLN3_HUMAN	155	21	48	47	56885	4.8	65000	4.9	
165	EGF-containing fibulin-like extracellular matrix protein 1 precursor	FBLN3_HUMAN	141	19	50	44	56885	4.8	70000	5.7	
166	EGF-containing fibulin-like extracellular matrix protein 1 precursor	FBLN3_HUMAN	121	17	61	43	56885	4.8	65000	5.6	
167	EGF-containing fibulin-like extracellular matrix protein 1 precursor	FBLN3_HUMAN	75	12	50	25	56885	4.8	70000	5.5	
168	EGF-containing fibulin-like extracellular matrix protein 1 precursor	FBLN3_HUMAN	164	24	59	50	56885	4.8	65000	5	
169	EGF-containing fibulin-like extracellular matrix protein 1 precursor	FBLN3_HUMAN	98	12	31	29	56885	4.8	70000	5.6	ECM structure
170	EGF-containing fibulin-like extracellular matrix protein 1 precursor	FBLN3_HUMAN	79	13	57	27	56885	4.8	64000	4.9	
171	EGF-containing fibulin-like extracellular matrix protein 1 precursor	FBLN3_HUMAN	142	19	61	48	56885	4.8	70000	5.6	
172	EGF-containing fibulin-like extracellular matrix protein 1 precursor	FBLN3_HUMAN	115	15	46	39	56885	4.8	65000	5.9	
173	EGF-containing fibulin-like extracellular matrix protein 1 precursor	FBLN3_HUMAN	85	9	41	23	56885	4.8	64000	4.9	
174	EGF-containing fibulin-like extracellular matrix protein 1 precursor	FBLN3_HUMAN	173	25	61	50	56885	4.8	64000	5	
175	EGF-containing fibulin-like extracellular matrix protein 1 precursor	FBLN3_HUMAN	165	21	41	47	56885	4.8	64000	5.5	
176	EGF-containing fibulin-like extracellular matrix protein 1 precursor	FBLN3_HUMAN	139	15	28	39	56885	4.8	70000	5.8	
177	EGF-containing fibulin-like extracellular matrix protein 1 precursor	FBLN3_HUMAN	105	12	24	32	56885	4.8	64000	5.5	
178	EGF-containing fibulin-like extracellular matrix protein 1 precursor	FBLN3_HUMAN	183	23	45	50	56885	4.8	67000	5.7	
179	EGF-containing fibulin-like extracellular matrix protein 1 precursor	FBLN3_HUMAN	158	19	38	43	56885	4.8	67000	5.5	
180	EGF-containing fibulin-like extracellular matrix protein 1 precursor	FBLN3_HUMAN	168	19	32	46	56885	4.8	67000	5.5	
181	EGF-containing fibulin-like extracellular matrix protein 1 precursor	FBLN3_HUMAN	138	18	44	40	56885	4.8	67000	6.1	
182	EGF-containing fibulin-like extracellular matrix protein 1 precursor	FBLN3_HUMAN	122	14	26	29	56885	4.8	65000	6.4	
183	EGF-containing fibulin-like extracellular matrix protein 1 precursor	FBLN3_HUMAN	172	25	62	50	56885	4.8	64000	5	
184	EGF-containing fibulin-like extracellular matrix protein 1 precursor	FBLN3_HUMAN	136	17	37	40	56885	4.8	65000	5.5	ECM structure
185	EGF-containing fibulin-like extracellular matrix protein 1 precursor	FBLN3_HUMAN	113	14	33	30	56885	4.8	65000	6.5	
186	EGF-containing fibulin-like extracellular matrix protein 1 precursor	FBLN3_HUMAN	146	22	66	50	56885	4.8	65000	5.1	
187	EGF-containing fibulin-like extracellular matrix protein 1 precursor	FBLN3_HUMAN	137	20	66	49	56885	4.8	65000	5.1	

Table 1. Continued

spot number	protein	accession name	Mascot score	peptides matched	peptides unmatched	sequence coverage %	theoretical MW Da	theoretical pI-value	experimental MW Da	experimental pI-value	comments
188	EGF-containing fibulin-like extracellular matrix protein 1 precursor	FBLN3_HUMAN	145	23	66	50	56885	4.8	64000	5.1	
189	EGF-containing fibulin-like extracellular matrix protein 1 precursor	FBLN3_HUMAN	149	23	63	50	56885	4.8	68000	4.9	
190	EGF-containing fibulin-like extracellular matrix protein 1 precursor	FBLN3_HUMAN	79	9	40	20	56885	4.8	55000	5.3	
191	EGF-containing fibulin-like extracellular matrix protein 1 precursor	FBLN3_HUMAN	93	14	44	34	56885	4.8	48000	5.3	
192	fibrillin-1 precursor	FBN1_HUMAN	59	12	27	4	332682	4.7	240000	4.6	ECM structure
193	fibrillin-1 precursor	FBN1_HUMAN	68	12	24	5	332682	4.7	240000	4.6	
194	fibronectin precursor	FN1_HUMAN	62	12	43	6	266034	5.4	260000	5.3	
195	fibronectin precursor	FN1_HUMAN	195	33	22	18	266034	5.4	260000	5.4	
196	fibronectin precursor	FN1_HUMAN	412	55	24	34	266034	5.4	260000	5.9	
197	fibronectin precursor	FN1_HUMAN	257	42	27	23	266034	5.4	260000	6	
198	fibronectin precursor	FN1_HUMAN	284	47	28	23	266034	5.4	260000	6.1	
199	fibronectin precursor	FN1_HUMAN	231	39	29	23	266034	5.4	260000	6.1	
200	fibronectin precursor	FN1_HUMAN	350	56	32	32	266034	5.4	260000	6.1	
201	fibronectin precursor	FN1_HUMAN	328	49	29	29	266034	5.4	260000	6.2	
202	fibronectin precursor	FN1_HUMAN	187	35	30	19	266034	5.4	260000	5.5	
203	fibronectin precursor	FN1_HUMAN	454	64	24	37	266034	5.4	260000	5.8	
204	fibronectin precursor	FN1_HUMAN	373	54	30	34	266034	5.4	260000	5.8	
205	fibronectin precursor	FN1_HUMAN	357	54	30	30	266034	5.4	260000	5.9	
206	fibronectin precursor	FN1_HUMAN	382	57	29	31	266034	5.4	260000	5.8	
207	fibronectin precursor	FN1_HUMAN	290	48	34	28	266034	5.4	260000	5.8	
208	fibronectin precursor	FN1_HUMAN	262	45	33	25	266034	5.4	260000	6	ECM structure
209	fibronectin precursor	FN1_HUMAN	331	50	30	30	266034	5.4	260000	6.2	
210	fibronectin precursor	FN1_HUMAN	358	55	33	33	266034	5.4	260000	6.3	
211	fibronectin precursor	FN1_HUMAN	339	49	26	30	266034	5.4	260000	6.6	
212	fibronectin precursor	FN1_HUMAN	484	68	24	36	266034	5.4	260000	5.5	
213	fibronectin precursor	FN1_HUMAN	365	55	24	31	266034	5.4	260000	5.6	
214	fibronectin precursor	FN1_HUMAN	282	45	24	24	266034	5.4	260000	6.6	
215	fibronectin precursor	FN1_HUMAN	339	54	34	30	266034	5.4	260000	5	
216	fibronectin precursor	FN1_HUMAN	435	64	26	34	266034	5.4	260000	5.6	
217	fibronectin precursor	FN1_HUMAN	439	63	27	37	266034	5.4	260000	5.6	
218	fibronectin precursor	FN1_HUMAN	172	30	25	17	266034	5.4	265000	5.1	
219	fibronectin precursor	FN1_HUMAN	381	55	30	33	266034	5.4	260000	4.8	
220	fibronectin precursor	FN1_HUMAN	410	60	28	31	266034	5.4	260000	4.9	
221	fibronectin precursor	FN1_HUMAN	281	44	25	25	266034	5.4	260000	5	
222	fibronectin precursor	FN1_HUMAN	379	60	30	31	266034	5.4	260000	5.1	
223	fibronectin precursor	FN1_HUMAN	138	33	46	19	266034	5.4	260000	4.6	
224	fibronectin precursor	FN1_HUMAN	104	18	15	10	266034	5.4	260000	4.7	
225	fibronectin precursor	FN1_HUMAN	172	34	37	20	266034	5.4	260000	4.8	
226	fibronectin precursor	FN1_HUMAN	198	34	24	19	266034	5.4	260000	4.8	
227	fibronectin precursor	FN1_HUMAN	126	25	27	14	266034	5.4	260000	4.6	
228	fibronectin precursor	FN1_HUMAN	457	64	25	34	266034	5.4	260000	4.9	
229	fibronectin precursor	FN1_HUMAN	262	43	27	23	266034	5.4	260000	4.7	
230	fibronectin precursor	FN1_HUMAN	154	29	28	16	266034	5.4	260000	4.7	
231	fibronectin precursor	FN1_HUMAN	357	57	30	30	266034	5.4	260000	4.4	
232	fibronectin precursor	FN1_HUMAN	310	46	23	26	266034	5.4	260000	4.4	
233	fibronectin precursor	FN1_HUMAN	148	30	29	15	266034	5.4	260000	4.3	
234	fibronectin precursor	FN1_HUMAN	217	35	25	21	266034	5.4	260000	4.5	
235	fibronectin precursor	FN1_HUMAN	219	37	26	19	266034	5.4	260000	4.6	
236	fibronectin precursor	FN1_HUMAN	98	19	21	10	266034	5.4	260000	4.6	
237	fibronectin precursor	FN1_HUMAN	194	33	23	18	266034	5.4	260000	4.4	
238	fibronectin precursor	FN1_HUMAN	173	29	19	15	266034	5.4	260000	5.4	
239	fibronectin precursor	FN1_HUMAN	127	19	37	10	266034	5.4	260000	6.6	
240	fibronectin precursor	FN1_HUMAN	84	17	21	10	266034	5.4	255000	5.9	
241	fibronectin precursor	FN1_HUMAN	70	13	40	7	266034	5.4	255000	5.2	
242	fibronectin precursor	FN1_HUMAN	145	36	52	20	266034	5.4	20000	5.4	

Table 1. Continued

spot number	protein	accession name	Mascot score	peptides matched	peptides unmatched	sequence coverage %	theoretical MW Da	theoretical pI-value	experimental MW Da	experimental pI-value	comments
243	fibronectin precursor	FINC_HUMAN	87	18	52	9	266034	5.4	255000	5.3	ECM structure
244	fibronectin precursor	FINC_HUMAN	116	17	29	8	266034	5.4	255000	5.8	
245	fibronectin precursor	FINC_HUMAN	107	20	57	11	266034	5.4	260000	5.2	
246	fibronectin precursor	FINC_HUMAN	155	28	25	15	266034	5.4	265000	5	
247	fibronectin precursor	FINC_HUMAN	176	35	34	19	266034	5.4	260000	5.7	
248	fibronectin precursor	FINC_HUMAN	98	18	50	9	266034	5.4	260000	5.3	
249	fibronectin precursor	FINC_HUMAN	144	29	34	18	266034	5.4	200000	5.7	
250	fibronectin precursor	FINC_HUMAN	114	16	28	8	266034	5.4	200000	5.8	
251	fibronectin precursor	FINC_HUMAN	63	11	27	5	266034	5.4	200000	5.8	
252	fibronectin precursor	FINC_HUMAN	77	13	33	7	266034	5.4	200000	5.9	
253	fibronectin precursor	FINC_HUMAN	98	25	36	13	266034	5.4	250000	5.6	
254	fibronectin precursor	FINC_HUMAN	110	16	32	9	266034	5.4	250000	5.7	
255	fibronectin precursor	FINC_HUMAN	93	15	33	8	266034	5.4	260000	6.3	
256	fibronectin precursor	FINC_HUMAN	227	43	45	27	266034	5.4	250000	5.5	
257	fibronectin precursor	FINC_HUMAN	104	29	54	16	266034	5.4	250000	5.1	
258	fibronectin precursor	FINC_HUMAN	117	32	53	17	266034	5.4	250000	5.1	
259	fibronectin precursor	FINC_HUMAN	128	31	41	16	266034	5.4	250000	5	
260	fibronectin precursor	FINC_HUMAN	58	10	31	5	266034	5.4	250000	4.4	
261	fibronectin precursor	FINC_HUMAN	102	15	28	8	266034	5.4	180000	5.7	
262	fibronectin precursor	FINC_HUMAN	90	18	59	10	266034	5.4	180000	5.1	
263	fibronectin precursor	FINC_HUMAN	80	18	27	10	266034	5.4	200000	5.2	
264	fibronectin precursor	FINC_HUMAN	89	14	35	8	266034	5.4	240000	5.3	
265	fibronectin precursor	FINC_HUMAN	173	37	49	22	266034	5.4	180000	5.5	
266	fibronectin precursor	FINC_HUMAN	74	21	41	12	266034	5.4	180000	5.4	
267	fibronectin precursor	FINC_HUMAN	79	14	41	8	266034	5.4	150000	5.7	
268	fibronectin precursor	FINC_HUMAN	108	19	52	10	266034	5.4	105000	5.6	
269	fibronectin precursor	FINC_HUMAN	74	24	60	15	266034	5.4	150000	5.5	
270	fibronectin precursor	FINC_HUMAN	68	24	61	14	266034	5.4	148000	5.5	
271	fibronectin precursor	FINC_HUMAN	82	25	61	15	266034	5.4	105000	5.5	
272	fibronectin precursor	FINC_HUMAN	82	18	66	9	266034	5.4	100000	5.5	
273	fibronectin precursor	FINC_HUMAN	53	9	28	5	266034	5.4	105000	5.4	ECM structure
274	fibulin-1 precursor	FBLN1_HUMAN	119	22	57	34	81315	5	110000	5	
275	fibulin-1 precursor	FBLN1_HUMAN	80	16	51	24	81315	5	110000	5	
276	fibulin-1 precursor	FBLN1_HUMAN	94	18	70	33	81315	5	110000	5	
277	fibulin-1 precursor	FBLN1_HUMAN	142	22	37	32	81315	5	105000	5.1	
278	fibulin-1 precursor	FBLN1_HUMAN	151	23	44	39	81315	5	105000	5.1	ECM structure
279	fibulin-1 precursor	FBLN1_HUMAN	161	26	61	46	81315	5	100000	5.1	
280	fibulin-1 precursor	FBLN1_HUMAN	152	25	47	38	81315	5	102000	5.2	
281	fibulin-1 precursor	FBLN1_HUMAN	142	25	59	41	81315	5	100000	5.2	
282	fibulin-1 precursor	FBLN1_HUMAN	121	18	41	32	81315	5	102000	5.2	
283	fibulin-1 precursor	FBLN1_HUMAN	87	16	63	28	81315	5	100000	5	
284	fibulin-1 precursor	FBLN1_HUMAN	89	17	65	31	81315	5	100000	5.1	
285	fibulin-1 precursor	FBLN1_HUMAN	108	16	34	27	81315	5	100000	5.3	
286	fibulin-1 precursor	FBLN1_HUMAN	85	18	71	31	81315	5	85000	5.2	
287	fibulin-1 precursor	FBLN1_HUMAN	88	16	52	27	81315	5	100000	5.3	
288	fibulin-1 precursor	FBLN1_HUMAN	111	14	60	25	81315	5	105000	5	
289	fibulin-1 precursor	FBLN1_HUMAN	88	18	67	31	81315	5	100000	5	
290	fibulin-1 precursor	FBLN1_HUMAN	88	15	39	22	81315	5	90000	5.4	BMP signaling pathway
291	folliculin-related protein 1 precursor	FSTL1_HUMAN	75	10	42	34	36103	5.3	47000	4.6	
292	folliculin-related protein 1 precursor	FSTL1_HUMAN	136	9	39	36	36103	5.3	46000	4.6	
293	folliculin-related protein 1 precursor	FSTL1_HUMAN	136	15	58	51	36103	5.3	46000	4.7	
294	folliculin-related protein 1 precursor	FSTL1_HUMAN	117	13	52	41	36103	5.3	45000	4.7	
295	folliculin-related protein 1 precursor	FSTL1_HUMAN	154	16	55	48	36103	5.3	45000	4.7	
296	folliculin-related protein 1 precursor	FSTL1_HUMAN	132	13	36	44	36103	5.3	45000	4.8	
297	folliculin-related protein 1 precursor	FSTL1_HUMAN	129	12	30	41	36103	5.3	40000	4.8	
298	folliculin-related protein 1 precursor	FSTL1_HUMAN	73	6	11	25	36103	5.3	39000	4.9	signal transduction/integrin mediated adhesion
299	galectin-3-binding protein precursor	LG3BP_HUMAN	63	11	56	23	66202	5	130000	5.8	
300	galectin-3-binding protein precursor	LG3BP_HUMAN	65	12	69	26	66202	5	90000	5.6	

Table 1. Continued

spot number	protein	accession name	Mascot score	peptides matched	peptides unmatched	sequence coverage %	theoretical MW Da	theoretical pI-value	experimental MW Da	experimental pI-value	comments
301	galectin-3-binding protein precursor	LG3BP_HUMAN	76	12	51	25	66202	5	90000	5.6	
302	galectin-3-binding protein precursor	LG3BP_HUMAN	85	13	53	28	66202	5	90000	5.7	
303	galectin-3-binding protein precursor	LG3BP_HUMAN	67	11	49	21	66202	5	100000	5.7	signal transduction/integrin mediated adhesion
304	galectin-3-binding protein precursor	LG3BP_HUMAN	68	8	53	18	66202	5	100000	6.2	
305	galectin-3-binding protein precursor	LG3BP_HUMAN	67	9	27	16	66202	5	110000	4.8	
306	galectin-3-binding protein precursor	LG3BP_HUMAN	68	10	37	20	66202	5	100000	5.9	
307	galectin-3-binding protein precursor	LG3BP_HUMAN	66	9	75	19	66202	5	105000	5.8	
308	galectin-3-binding protein precursor	LG3BP_HUMAN	69	11	46	21	66202	5	110000	4.8	
309	galectin-3-binding protein precursor	LG3BP_HUMAN	130	17	40	33	66202	5	105000	4.4	
310	galectin-3-binding protein precursor	LG3BP_HUMAN	180	21	39	38	66202	5	100000	4.4	
311	galectin-3-binding protein precursor	LG3BP_HUMAN	196	24	51	43	66202	5	100000	4.4	
312	galectin-3-binding protein precursor	LG3BP_HUMAN	134	20	67	37	66202	5	100000	4.5	
313	galectin-3-binding protein precursor	LG3BP_HUMAN	154	21	59	37	66202	5	100000	4.5	
314	galectin-3-binding protein precursor	LG3BP_HUMAN	137	20	64	40	66202	5	100000	4.5	
315	galectin-3-binding protein precursor	LG3BP_HUMAN	147	21	65	40	66202	5	100000	4.6	
316	galectin-3-binding protein precursor	LG3BP_HUMAN	96	14	41	28	66202	5	100000	4.6	
317	galectin-3-binding protein precursor	LG3BP_HUMAN	80	11	34	22	66202	5	100000	4.6	
318	galectin-3-binding protein precursor	LG3BP_HUMAN	84	11	31	22	66202	5	100000	4.7	
319	gelsolin precursor	GELS_HUMAN	129	18	36	31	86043	5.9	85000	6.1	structural
320	gelsolin precursor	GELS_HUMAN	136	17	26	27	86043	5.9	75000	6.3	
321	insulin-like growth factor-binding protein 4 precursor	IBP4_HUMAN	58	6	26	26	29113	7	30000	6.5	signal transduction
322	insulin-like growth factor-binding protein 4 precursor	IBP4_HUMAN	69	7	30	33	29113	7	30000	6.5	
323	insulin-like growth factor-binding protein 4 precursor	IBP4_HUMAN	71	7	28	33	29113	7	30000	6.5	
324	insulin-like growth factor-binding protein 4 precursor	IBP4_HUMAN	74	7	25	33	29113	7	30000	6.6	signal transduction
325	insulin-like growth factor-binding protein 4 precursor	IBP4_HUMAN	66	7	34	33	29113	7	30000	6.6	
326	insulin-like growth factor-binding protein 6 precursor	IBP6_HUMAN	58	5	18	27	26219	9.8	30000	5.6	signal transduction
327	insulin-like growth factor-binding protein 6 precursor	IBP6_HUMAN	59	6	36	27	26219	9.8	30000	5.9	
328	insulin-like growth factor-binding protein 7 precursor	IBP7_HUMAN	58	7	30	27	30138	9.6	35000	6.6	regulation of cell growth
329	interleukin-6 precursor	IL6_HUMAN	58	5	17	28	23931	6.2	20000	5.6	cytokine/growth factor
330	laminin subunit beta-1 precursor	LAMB1_HUMAN	173	37	53	26	205178	4.7	250000	4.7	basement membrane structure
331	laminin subunit beta-2 precursor	LAMB2_HUMAN	209	38	49	28	202982	6.1	250000	6.5	basement membrane structure
332	laminin subunit gamma-1 precursor	LAMC1_HUMAN	193	35	54	29	183195	4.9	250000	4.8	basement membrane structure
333	laminin subunit gamma-1 precursor	LAMC1_HUMAN	246	41	48	34	183195	4.9	250000	4.8	
334	laminin subunit gamma-1 precursor	LAMC1_HUMAN	158	32	55	26	183195	4.9	250000	4.8	
335	laminin subunit gamma-1 precursor	LAMC1_HUMAN	206	37	51	31	183195	4.9	250000	4.8	
336	laminin subunit gamma-1 precursor	LAMC1_HUMAN	191	34	51	29	183195	4.9	250000	4.9	
337	latent-transforming growth factor beta-binding protein 2 precursor	LTBP2_HUMAN	150	32	44	19	204059	5	260000	5.1	structural/TGFb signaling
338	latent-transforming growth factor beta-binding protein 2 precursor	LTBP2_HUMAN	100	27	57	17	204059	5	260000	5.1	
339	latent-transforming growth factor beta-binding protein 2 precursor	LTBP2_HUMAN	164	34	48	22	204059	5	260000	5.2	
340	latent-transforming growth factor beta-binding protein 2 precursor	LTBP2_HUMAN	70	22	58	15	204059	5	260000	5.2	structural/TGFb signaling
341	latent-transforming growth factor beta-binding protein 3 precursor	LTBP3_HUMAN	77	18	54	18	146451	5.7	250000	5.4	structural/TGFb signaling
342	latent-transforming growth factor beta-binding protein 3 precursor	LTBP3_HUMAN	136	26	60	27	146451	5.7	249000	5.4	
343	latent-transforming growth factor beta-binding protein 3 precursor	LTBP3_HUMAN	61	7	20	7	146451	5.7	250000	5.4	

Table 1. Continued

spot number	protein	accession name	Mascot score	peptides matched	peptides unmatched	sequence coverage %	theoretical MW Da	theoretical pI-value	experimental MW Da	experimental pI-value	comments
344	lysyl oxidase homologue 2 precursor	LOXL2_HUMAN	65	10	62	15	88778	5.9	100000	5.9	cell adhesion/redox regulation/ metal binding
345	lysyl oxidase homologue 2 precursor	LOXL2_HUMAN	67	10	59	15	88778	5.9	100000	6	cell adhesion/redox regulation/ metal binding
346	plasma retinol-binding protein precursor	RETBP_HUMAN	57	4	27	30	23337	5.7	20000	5.5	vitA binding
347	SPARC precursor	SPARC_HUMAN	74	8	15	24	35465	4.6	39000	4.6	matricellular
348	SPARC precursor	SPARC_HUMAN	84	10	25	27	35465	4.6	38000	4.6	
349	SPARC precursor	SPARC_HUMAN	152	17	39	48	35465	4.6	37000	4.7	
350	SPARC precursor	SPARC_HUMAN	142	15	34	48	35465	4.6	37000	4.7	
351	SPARC precursor	SPARC_HUMAN	123	14	40	48	35465	4.6	37000	4.8	
352	SPARC precursor	SPARC_HUMAN	79	9	20	27	35465	4.6	37000	4.8	
353	sulphydryl oxidase 1 precursor	QSOX1_HUMAN	75	12	32	18	83324	9.9	80000	6.1	redox homeostasis
354	sulphydryl oxidase 1 precursor	QSOX1_HUMAN	70	7	22	11	83324	9.9	80000	6.4	
355	sulphydryl oxidase 1 precursor	QSOX1_HUMAN	57	10	40	15	83324	9.9	74000	6.4	
356	sulphydryl oxidase 1 precursor	QSOX1_HUMAN	100	13	28	21	83324	9.9	74000	6.5	
357	translationally controlled tumor protein	TCTP_HUMAN	68	6	18	36	19697	4.7	21000	4.9	Calcium binding microtubule stabilization
358	trypsin-2 precursor	TRY2_HUMAN	64	7	27	37	26927	4.6	30000	4.9	protease

^a Protein classification was based on GO and “secreted” is defined as follows: proteins have a signal peptide and are characterised by at least one of the following GO terms: secreted, extracellular space, extracellular matrix, exocytosis. The only exceptions are (a) 14-3-3 protein sigma which does not have a signal peptide but may be secreted by a non classical secretory pathway according to GO and (b) cathepsin B and cathepsin Z precursors which have a signal peptide but no other reported GO term related to their potential secretion. Nevertheless, for cathepsin B, literature data support its presence in the extracellular space.⁴⁹ The protein accession name (Swiss-Prot), theoretical and observed MW and pI, identification parameters (Mascot score, coverage, matched/unmatched peptides) and few indicative comments on the function of these proteins are provided.

Dickkopf-related protein 3 precursor, 14-3-3 protein sigma etc. (Table 1 and Figure 2).

Notably, of the rest identified proteins a large part were proteins of the cell surface and/or plasma membrane according to GO (at least in their full length form such as HLA antigens, cadherin, tyrosine-protein kinase-like 7, Calsyntenin-1, amyloid-like protein 2, Semaphorine 4B, protein jagged-1, ezrin, Rab GDP dissociation inhibitor beta, brain acid soluble protein 1, chloride intracellular channel proteins 1 and 4 and others) with the rest being cytosolic, lysosomal, nuclear, endoplasmic reticulum and/or cytoskeletal proteins potentially being released due to cell death (Supplementary Table-T24 CM Map, Supporting Information).

Analysis of Protein Differential Expression in T24 and T24M Conditioned Media. A comparison of the expression levels of the proteins in the conditioned media of the two cell lines was conducted, using a total of 5 gels per category corresponding to at least two different passage numbers per cell line. Representative gel images are shown in Figure 3. Nine protein spots were found to be differentially expressed at statistically significant levels in the two cell lines (Table 2). Specifically, proteins up-regulated in the T24M cells included SPARC, tPA, clusterin, PDI, cathepsin L1, carboxypeptidase A4, heat shock cognate protein 71, BASP1 and galectin 3 binding protein. Of those SPARC, tPA, clusterin, cathepsin L1 and galectin 3BP are bona fide secreted proteins according to gene ontology.

The differential expression of SPARC, tPA and clusterin was further confirmed by Western blot analysis using cell line conditioned media preparations that were different from the ones employed in the 2DE analysis. In the case of SPARC, two bands were recognized by the Ab in the media: A protein band of approximately 40 kDa corresponding to the expected size of the glycosylated protein¹² as well as a higher MW band at 70 kDa (Figure 4A). Both of these bands appeared up-regulated in T24M cells compared to T24 cells by 68% and 81% ($p < 0.05$ Student’s *t*-test) respectively. In the case of tPA and clusterin, bands at the expected MW were similarly observed and in accordance to 2DE, upregulated in the T24M cells by 90 and 49% ($p < 0.05$ Student’s *t*-test), respectively (Figure 4B,C).

SPARC Affects T24M Cell Motility. SPARC has been implicated in many types of neoplasia such as prostate, colon and breast cancer.¹³ To get some initial insight into whether this protein may be also involved in bladder cancer aggressiveness, *in vitro* blocking experiments were conducted involving transwell migration assays of T24M cells in the presence of SPARC specific Ab or isotype IgG1 control Ab. As shown (Figure 5), motility of T24M cells toward their CM decreases when either cells ($27\% \pm 18$, $p = 0.01$) or media ($75\% \pm 11$, $p < 0.01$, Student’s *t*-test) were preincubated with the SPARC-Ab; nevertheless, no additive effect was observed upon blocking of SPARC in both media and cells ($48\% \pm 5$ $p < 0.01$ Student’s *t*-test) (Figure 5). In contrast, there was no significant effect on T24M cell migration in the presence of the IgG1 antibody, supporting the specificity of SPARC-Ab observed effect.

Discussion

The term “secretome” was first employed by Tjalsma et al¹⁴ in a genome based global survey on secreted proteins of *Bacillus subtilis*. Nevertheless, major obstacle in the study of these proteins is their presence at usually low concentrations (ng/mL range i.e. in the case of cytokines). Recently advancements in proteomic technologies have facilitated to some extent the study of these

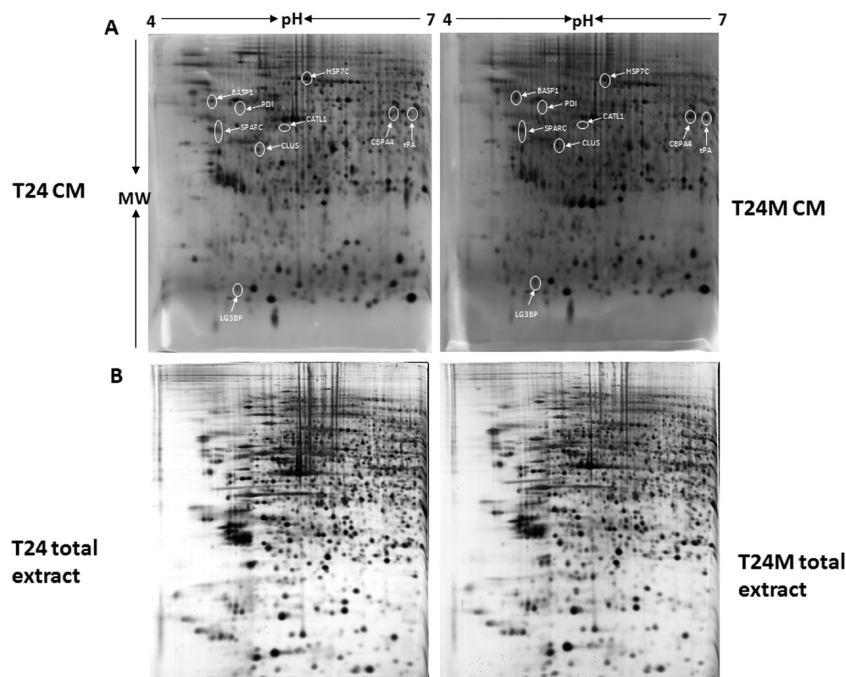


Figure 3. Differentially expressed proteins in CM of T24M versus T24 bladder cancer cell lines. (A) Representative 2D gels of T24 CM (left) and T24M CM (right). Differentially expressed spots (over 2 fold and $p < 0.05$, 5 gels per category corresponding to at least 2 biological replicates) are shown. Swiss-Prot accession names are provided. (B) 2DE images of respective total cell extracts of T24 (left) and T24M (right) depicted as a control to show their overall difference with the CM proteomic patterns. In all cases, 100 μ g of total protein were analyzed; 17 cm linear strips pH range 4–7 (Biorad) were employed and spot detection by silver staining was performed. Protein identification was conducted by MALDI-TOF-MS PMF and LC-MS/MS analysis.

proteins (reviewed in ref 4). In brief, 2DE-based^{5,15–17} as well as comprehensive LC-MS/MS approaches^{9,18–23} have been applied for the study of cell secretome of a variety of cancer cell types including prostate, breast, ovarian, lung, renal and others. Various classical extracellular proteins (CXCL1, interleukin 8, galectin 3 binding protein, cathepsin D, pro-MMP7 and others) were found differentially expressed between cancer cells under study and controls; findings were, in some cases, confirmed by immunoassays in serum samples.⁴ Collectively, the existing data support the potential of using the cell secretome as a source of putative disease biomarkers and means for investigation of mechanisms of cell motility and aggressiveness.

We employed the TCA-NLS protein precipitation protocol by Chevallet et al.⁵ in combination to 2DE for the enrichment of secreted proteins from bladder cancer cells. This protocol appears to reproducibly provide high recovery rates while maintaining compatibility with 2DE analysis. Using stringent identification criteria, a total of 358 detected spots (46 different gene products, 51% of the total identified protein spots) corresponded to secreted proteins (according to GO). Among those, as expected, were multiple structural proteins of the extracellular matrix (such as fibronectin, collagen, fibulin, laminin, fibrillin), complement pathway proteins (complement C1r, C1s, C3, complement factor B and H), proteases (cathepsin L1, cathepsin D, cathepsin Z, carboxypeptidase A4, tPA, MMP2) and other enzymes (Lysyl oxidase homologue 2, sulfhydryl oxidase 1) and growth factors and cytokines (interleukin 6, insulin-like growth factor-binding protein 4, stem cell growth factor etc), frequently encountered in multiple isoforms (Table 1). Notably, a large number of the CM identified proteins are classified as cell membrane components involved in cell communication and adhesion. Even though the presence of

cytoplasmic proteins was still evident, there is a very clear and significant enrichment for secreted proteins supporting the effectiveness of this preparation protocol and the potential employment of the reported 2-DE proteomic map as a reference for future secretome studies. Notably, comprehensive proteomic databases of cell line conditioned media are generally lacking.

The objective of this study was to identify secreted factors that may be involved in bladder cancer cell aggressiveness. Toward that end we employed the aggressive T24M in comparison to their parental and less aggressive T24 cells.³ Interestingly, T24M CM increased T24 cells motility *in vitro*, enhancing the hypothesis that secreted factors are involved in the acquisition of the aggressive phenotype. Of the differentially expressed secreted proteins in the two cell lines, SPARC, tPA, clusterin, galectin 3 binding protein, cathepsin L1 and carboxypeptidase A4 have been implicated in cancer progression for other types of malignancies.^{24–30}

In brief, SPARC is a matricellular Ca^{2+} binding glycoprotein attributed a variety of functions.³¹ It is a counter-adhesive molecule,³² inhibits the production of basement membrane components,³³ increases the permeability of endothelial barriers,³⁴ induces the production and activation of matrix metalloproteinases,^{35,36} and affects growth factor signaling.³¹ Through these functions SPARC has been placed at the crossroad of multiple cancer hallmarks such as proliferation, migration and angiogenesis. Notably, existing evidence regarding specific functions of SPARC in cancer, is frequently contradictory. For example, high levels of SPARC in a variety of malignant tumors, such as melanoma, gliomas, pancreatic cancer, osteosarcoma, and thyroid cancer, have been associated with poor prognosis.^{13,24} On the contrary, in other cases such as neuroblastomas and ovarian cancer,^{13,24} SPARC expression

Table 2. Differentially Expressed Proteins (over 2 fold and $p < 0.05$), in T24M versus T24 CM Following Proteomics and Image Analysis^a

protein	accession number	Mascot Score	peptides matched	peptides unmatched	sequence coverage %	theoretical MW(kDa)/pI	experimental MW(kDa)/pI	T24CM (density in ppm) \pm SD	T24MCM (density in ppm) \pm SD	T24MCM/T24CM ratio	p value
BASP1 (Brain Acid Soluble Protein 1)	P80723	87 ^b	3 (LC-MS/MS)	na	18.9	23/4.6	75/4.4	1410 \pm 430	2940 \pm 290	2.1	0.01
Carboxypeptidase A4	Q9UI42	82 ^b	3 (LC-MS/MS)	na	5.8	47/6.2	50/6.2	420 \pm 90	4540 \pm 890	10.8	0.01
Cathepsin L1 precursor	P07711	69	11	32	30	38/5.2	40/5.1	370 \pm 140	760 \pm 180	2.1	0.04
Clusterin	P10909	75	6	24	20	53/5.9	37/4.9	700 \pm 80	1560 \pm 250	2.2	0.02
Galectin 3 binding protein	Q08380	91	11	26	22	66/5	20/4.6	90 \pm 20	420 \pm 90	4.7	0.02
Heat shock cognate protein 71	P11142	139	11	30	29	71/5.4	100/5.4	1230 \pm 530	2650 \pm 230	2.2	0.03
Protein Disulfide Isomerase precursor	P07237	59	5	11	9	57/4.8	70/4.7	290 \pm 60	740 \pm 160	2.6	0.03
SPARC (Secreted Protein Acidic Rich in Cysteine)	P09486	61	7	16	21	35/4.6	40/4.5	510 \pm 130	1170 \pm 120	2.3	0.01
tPA (tissue type plasminogen activator)	P00750	84 ^b	1 (LC-MS/MS)	na	2.3	63/8.1	50/6.5	940 \pm 210	4500 \pm 990	4.8	0.02

^a Protein accession name (Swiss-Prot) Identification parameters and fold difference are provided. Location of proteins in the gel is shown in Figure 3. ^b Respective sequence scores for MS/MS identifications were 20 for BASP1, 18 for Carboxypeptidase A4 and 10 for tPA.

has been associated with good prognosis. Along the same lines, SPARC has in cases been attributed a tumor suppressor, and others, a tumor promoter role.³¹ The mechanism by which SPARC exerts its functions remains largely unknown even though it is generally believed that interactions with growth factor receptors, ECM components and integrins should play a central role. In general, this plurality of SPARC functions is considered reflective of cell type and context differences in the biological systems under investigation in different studies; nevertheless, it may also be related to the presence of the protein in different isoforms. SPARC has been recently found to be the substrate of various proteases giving rise to distinct degradation fragments.^{37,38} In our study, SPARC was detected in multiple protein spots during the 2DE analysis (spots 347–352; Figure 2) and additionally using an Ab recognizing the full length protein, 2 protein bands were detected in 1DE analysis of cell secretome: one at the expected MW (40 kDa) and a larger form at approximately 70 kDa. Both of these bands were upregulated in T24M cells CM and preliminary studies from our lab support that both are also detected in urine from bladder cancer patients. The difference between these isoforms is under investigation, nevertheless does not seem to be related to potential extensive S–S bonding since protein reduction and alkylation with various reagents prior to gel loading did not affect the protein motility (data not shown).

In the case of bladder cancer as supported herein by the *in vitro* findings, SPARC may be involved in induction of cell motility. A preliminary *in vivo* investigation indicated that SPARC is also expressed in tumors generated following injection of T24M cells in NOD/SCID mice (Supplementary Figure 2, Supporting Information). Further detailed *in vivo* investigation and confirmation of this finding is undoubtedly required, nevertheless our findings provide the initial evidence that such studies are well justified in the case of bladder cancer.

Besides SPARC, various proteases were also found to be differentially expressed in T24M cells: Cathepsin L1 is a lysosomal cysteine protease, secreted by many malignant cells in culture²⁸ and presumably mediating degradation of collagen, laminin, elastin and other structural proteins of the extracellular matrix.²⁸ tPA converts the abundant, but inactive zymogen plasminogen to plasmin controlling plasmin-mediated proteolysis, and thereby playing an important role in tissue remodeling and cell migration.³⁹ Carboxypeptidase A4 is a zinc dependent metallo -carboxypeptidase whose expression has been linked to prostate cancer aggressiveness.^{29,40}

In agreement to our findings, cathepsin L activity has been found to be elevated in bladder cancer cell lines, tissue as well as urine of bladder cancer patients.^{41–43} Along the same lines, previous studies have shown that the levels of tPA in combination to its inhibitor (-PAI-1) were increased in bladder cancer tissue in comparison to normals even though free tPA was lower in tumor tissue.⁴⁴ Existing data relating expression of Carboxypeptidase A4 with bladder cancer are not available to the best of our knowledge.

Clusterin was also found to be upregulated in the T24M CM. Of note, this protein has been identified as a mediator of SPARC activity in melanoma cells, with diminished SPARC correlating with reduction of clusterin levels, and vice versa.⁴⁵ In agreement to this finding, clusterin was detected in our study with similar expression trends to SPARC (e.g., both proteins were overexpressed in T24M cells), enhancing the hypothesis for a potential functional correlation between the two proteins. Interestingly and in line with our observations, clusterin has also been

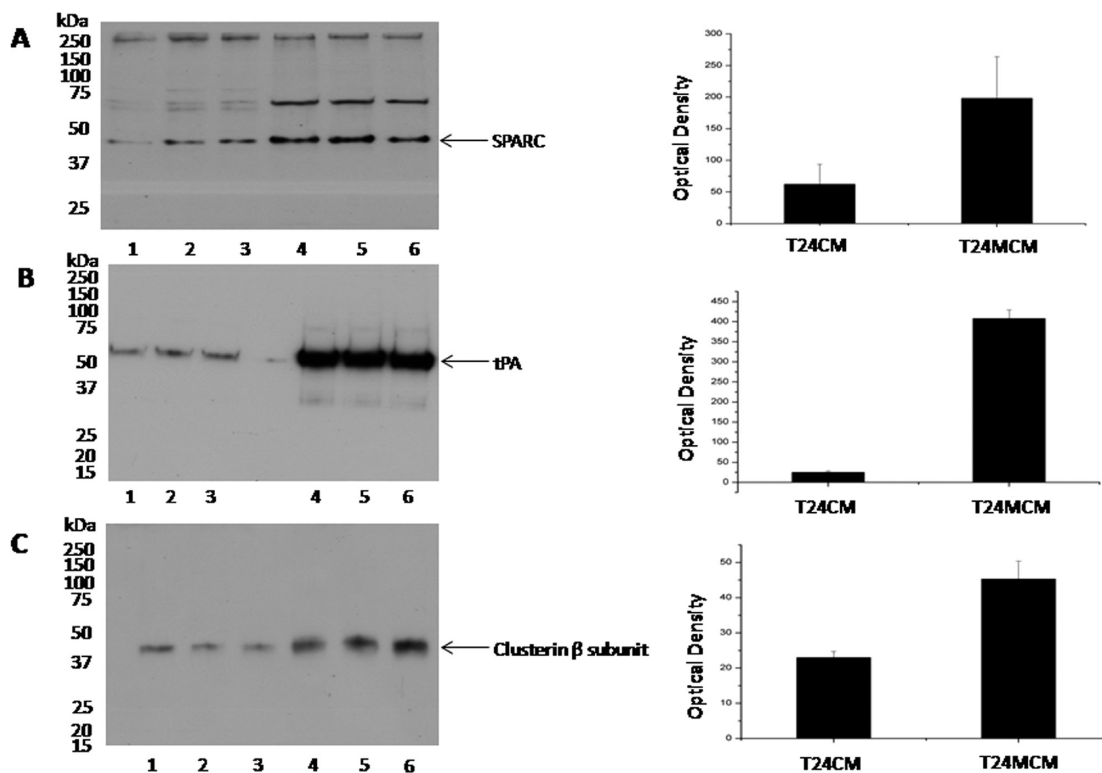


Figure 4. Western blot analysis of (A) SPARC, (B) tPA and (C) clusterin β subunit showing overexpression of these proteins in the T24M CM compared to T24 CM, in accordance to the 2DE findings ($p < 0.05$ Student's t -test). Notably different CM preparations to the ones used for the 2DE analysis were employed. Ten micrograms of total protein from separate CM preparations (eg corresponding to biological replicates) were loaded per lane and equal loading was confirmed by Coomassie staining of replicate gels and Ponceau S staining of the membrane. In all cases, lanes 1–3 and 4–6 correspond to conditioned media of T24 and T24M respectively. Graphical representation (densitometry analysis) of the results (mean \pm SD) is also shown. In the case of SPARC the analysis of the 40 kDa band (expected size of the glycosylated SPARC¹²) is shown, nevertheless an upregulation of the 70 kDa band in T24M cells compared to T24 cells (81% , 133 ± 18 , 25 ± 1 , $p < 0.05$ Student's t -test) could also be observed.

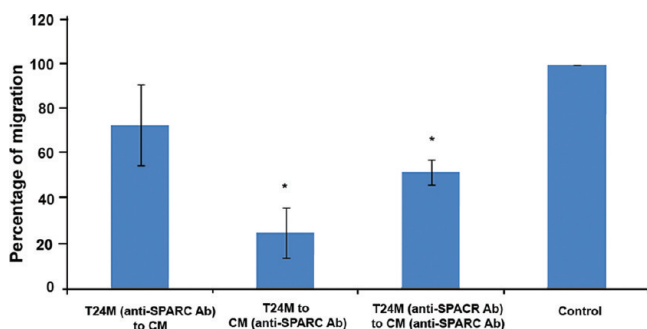


Figure 5. *In vitro* blockage of SPARC results in decrease of bladder cancer cell motility. Percentage of migrated cells (normalized to the migration of the nontreated cells to non-treated CM which was set to 100%) following incubation (30 min–4 °C) of T24M cells, their CM or both with specific mouse antihuman SPARC or control Ab is shown. In all cases 50 000 cells were initially plated, migration was allowed for 6 h and migrated cells counted as described in Figure 1. Data are presented as the mean \pm SD and were analyzed by Student's t -test.

recently found to be upregulated in urine samples of high grade bladder cancer in comparison to low grade and benign-normal samples.⁴⁶

Galectin 3 binding protein, also designated as Mac-2BP or 90K, is a secreted glycoprotein that binds galectins 1, 3, and 7. Overexpression of this protein has been implicated with cancer aggressiveness, metastasis, shorter survival, and reduced response to chemotherapy in different types of malignancies such

as breast and lung cancers,⁴⁷ nevertheless no such evidence for bladder cancer is available yet. Consistent with the secretome findings presented herein, preliminary studies from our lab support the detection of G3BP in urine from bladder cancer patients following protein enrichment through chromatographic approaches.

Conclusion

Collectively with the current study, we report a comprehensive secretome 2DE map along with the identification of secreted proteins potentially involved in the acquisition of the aggressive phenotype for bladder cancer cells. According to our findings, SPARC may be playing a key role in this process, possibly through its interactions with the ECM components, as well as regulation of proteases and/or modulation of angiogenesis and growth factors. To date there have not been reports to the best of our knowledge implicating this protein with aggressive bladder cancer with the exception of a publication from Yamanaka et al. studying the m-RNA levels of SPARC in cancer and normal urothelium.⁴⁸ More efforts should be made to elucidate how this molecule interacts within the cancer microenvironment promoting cell motility and aggressiveness. Investigation of the differences between the SPARC isoforms and detailed analysis of their expression would be a logical next step in this direction. In addition, the analysis of the expression of SPARC and the other secreted proteins presented herein in urine of bladder cancer patients by the use of sensitive assays is well justified and currently pursued.

Abbreviations: CM, conditioned medium; FM, fresh medium; SFM, serum and phenol red free medium; IEF, isoelectric focusing; SPARC, secreted protein acidic and rich in cysteine; THF, tetra hydro furan; NLS, N-lauroyl sarcosine; LG3BP, galectin 3 binding protein; tPA, tissue type plasminogen activator; BASP 1, brain acid soluble protein 1; CXCL1, C-X-C motif chemokine 1; PDI, protein disulfide isomerase.

Acknowledgment. This work was supported by the DECanBio FP7 project (201333). M.M. was supported by a Short Term Scientific Mission of the EuroKUP COST Action.

Supporting Information Available: Figure S1: 2DE map of T24 conditioned medium (Image is the same as in Figure 2; in this case though all spots processed for identification are shown). One thousand three hundred and eighty four spots were picked, which resulted in the identification of 694 spots (numbers correspond to spot numbers of Supplementary T24CM map Table). Figure S2: Expression of SPARC protein at T24M tumor sections. SPARC expression was evaluated by immunohistochemistry at sections from tumors developed in NOD/SCID mice after subcutaneous transplantation as described in materials and methods and ref 3. Tumors were excised from mice one month after the initial injection of T24M cells. Immunohistochemistry was performed using anti-SPARC or IgG1 isotype control antibodies. Images were taken under a light microscope at 20× magnification. Supplementary Table-T24CM Map: Table with all protein identifications received from the 2DE analysis of T24 CM. (Secreted proteins are marked in red and shown separately in Table 1.) A box plot analysis showing the distribution of proteins according to cellular compartment (GO) is also provided in the bottom of the table. Supplementary Table Annotated Spectra T24CM map PMF 1: Peak lists and spectra from PMF identifications of T24CM map (secreted proteins according to GO). Supplementary Table Annotated Spectra T24CMmap PMF 2: Peak lists and spectra from PMF identifications of T24CM map (rest (non secreted) proteins of map). Supplementary Table Annotated Spectra Differential Expression: This file has 3 xls sheets: (a) "Annotated spectra from differentially expressed spots PMF"; containing all peak lists and spectra from PMF identifications of differentially expressed protein spots; (b) "MS-MS spectra 1peptide ID" depicting MS-MS spectra and fragmentation tables in case of 1 peptide ID of differentially expressed protein spots; and (c) "Differentially Expressed spots LC-MS-MS", containing detailed LC-MS/MS identification information for differentially expressed spots, as applicable. This material is available free of charge via the Internet at <http://pubs.acs.org>.

References

- Dinney, C. P.; McConkey, D. J.; Millikan, R. E.; Wu, X.; Bar-Eli, M.; Adam, L.; Kamat, A. M.; Siefker-Radtke, A. O.; Tuziak, T.; Sabichi, A. L.; Grossman, H. B.; Benedict, W. F.; Czerniak, B. Focus on bladder cancer. *Cancer Cell* **2004**, *6*, 111–116.
- Crallan, R. A.; Georgopoulos, N. T.; Southgate, J. Experimental models of human bladder carcinogenesis. *Carcinogenesis* **2006**, *27*, 374–381.
- Makridakis, M.; Gagos, S.; Petrolekas, A.; Roubelakis, M. G.; Bitsika, V.; Stravodimos, K.; Pavlakis, K.; Anagnou, N. P.; Coleman, J.; Vlahou, A. Chromosomal and proteome analysis of a new T24-based cell line model for aggressive bladder cancer. *Proteomics* **2009**, *9*, 287–298.
- Xue, H.; Lu, B.; Lai, M. The cancer secretome: a reservoir of biomarkers. *J. Transl. Med.* **2008**, *6*, 52.
- Chevallet, M.; Diemer, H.; Van Dorsselaar, A.; Villiers, C.; Rabilloud, T. Toward a better analysis of secreted proteins: the example of the myeloid cells secretome. *Proteomics* **2007**, *7*, 1757–1770.
- Faca, V. M.; Hanash, S. M. In-depth proteomics to define the cell surface and secretome of ovarian cancer cells and processes of protein shedding. *Cancer Res.* **2009**, *69*, 728–730.
- Kulasingham, V.; Diamandis, E. P. Tissue culture-based breast cancer biomarker discovery platform. *Int. J. Cancer* **2008**, *123*, 2007–2012.
- Hathout, Y. Approaches to the study of the cell secretome. *Expert Rev. Proteomics* **2007**, *4*, 239–248.
- Kawanishi, H.; Matsui, Y.; Ito, M.; Watanabe, J.; Takahashi, T.; Nishizawa, K.; Nishiyama, H.; Kamoto, T.; Mikami, Y.; Tanaka, Y.; Jung, G.; Akiyama, H.; Nobumasa, H.; Guilford, P.; Reeve, A.; Okuno, Y.; Tsujimoto, G.; Nakamura, E.; Ogawa, O. Secreted CXCL1 is a potential mediator and marker of the tumor invasion of bladder cancer. *Clin. Cancer Res.* **2008**, *14*, 2579–2587.
- Lin, C. Y.; Tsui, K. H.; Yu, C. C.; Yeh, C. W.; Chang, P. L.; Yung, B. Y. Searching cell-secreted proteomes for potential urinary bladder tumor markers. *Proteomics* **2006**, *6*, 4381–4389.
- Roubelakis, M. G.; Pappa, K. I.; Bitsika, V.; Zagoura, D.; Vlahou, A.; Papadaki, H. A.; Antsaklis, A.; Anagnou, N. P. Molecular and proteomic characterization of human mesenchymal stem cells derived from amniotic fluid: comparison to bone marrow mesenchymal stem cells. *Stem Cells Dev* **2007**, *16*, 931–952.
- Kaufmann, B.; Muller, S.; Hanisch, F. G.; Hartmann, U.; Paulsson, M.; Maurer, P.; Zaucke, F. Structural variability of BM-40/SPARC/osteonectin glycosylation: implications for collagen affinity. *Glycobiology* **2004**, *14*, 609–619.
- Podhajcer, O. L.; Benedetti, L. G.; Girotti, M. R.; Prada, F.; Salvatierra, E.; Llera, A. S. The role of the matricellular protein SPARC in the dynamic interaction between the tumor and the host. *Cancer Metastasis Rev.* **2008**, *27*, 691–705.
- Tjalsma, H.; Bolhuis, A.; Jongbloed, J. D.; Bron, S.; van Dijk, J. M. Signal peptide-dependent protein transport in *Bacillus subtilis*: a genome-based survey of the secretome. *Microbiol. Mol. Biol. Rev.* **2000**, *64*, 515–547.
- Huang, L. J.; Chen, S. X.; Huang, Y.; Luo, W. J.; Jiang, H. H.; Hu, Q. H.; Zhang, P. F.; Yi, H. Proteomics-based identification of secreted protein dihydrodiol dehydrogenase as a novel serum markers of non-small cell lung cancer. *Lung Cancer* **2006**, *54*, 87–94.
- Lou, X.; Xiao, T.; Zhao, K.; Wang, H.; Zheng, H.; Lin, D.; Lu, Y.; Gao, Y.; Cheng, S.; Liu, S.; Xu, N. Cathepsin D is secreted from M-BE cells: its potential role as a biomarker of lung cancer. *J. Proteome Res.* **2007**, *6*, 1083–1092.
- Sarkissian, G.; Fergelot, P.; Lamy, P. J.; Pataud, J. J.; Culine, S.; Jouin, P.; Rioux-Leclercq, N.; Darboret, B. Identification of pro-MMP-7 as a serum marker for renal cell carcinoma by use of proteomic analysis. *Clin. Chem.* **2008**, *54*, 574–581.
- Yamashita, R.; Fujiwara, Y.; Ikari, K.; Hamada, K.; Otomo, A.; Yasuda, K.; Noda, M.; Kaburagi, Y. Extracellular proteome of human hepatoma cell, HepG2 analyzed using two-dimensional liquid chromatography coupled with tandem mass spectrometry. *Mol. Cell. Biochem.* **2007**, *298*, 83–92.
- Mauri, P.; Scarpa, A.; Nascimbeni, A. C.; Benazzi, L.; Parmagnani, E.; Mafficini, A.; Della Peruta, M.; Bassi, C.; Miyazaki, K.; Sorio, C. Identification of proteins released by pancreatic cancer cells by multidimensional protein identification technology: a strategy for identification of novel cancer markers. *FASEB J.* **2005**, *19*, 1125–1127.
- Sardana, G.; Marshall, J.; Diamandis, E. P. Discovery of candidate tumor markers for prostate cancer via proteomic analysis of cell culture-conditioned medium. *Clin. Chem.* **2007**, *53*, 429–437.
- Sardana, G.; Jung, K.; Stephan, C.; Diamandis, E. P. Proteomic analysis of conditioned media from the PC3, LNCaP, and 22Rv1 prostate cancer cell lines: discovery and validation of candidate prostate cancer biomarkers. *J. Proteome Res.* **2008**, *7*, 3329–3338.
- Mbeunkui, F.; Metge, B. J.; Shevde, L. A.; Pannell, L. K. Identification of differentially secreted biomarkers using LC-MS/MS in isogenic cell lines representing a progression of breast cancer. *J. Proteome Res.* **2007**, *6*, 2993–3002.
- Kulasingham, V.; Diamandis, E. P. Proteomics analysis of conditioned media from three breast cancer cell lines: a mine for biomarkers and therapeutic targets. *Mol. Cell. Proteomics* **2007**, *6*, 1997–2011.
- Tai, I. T.; Tang, M. J. SPARC in cancer biology: its role in cancer progression and potential for therapy. *Drug Resist. Updates* **2008**, *11*, 231–246.
- Hackel, C.; Czerniak, B.; Ayala, A. G.; Radig, K.; Roessner, A. Expression of plasminogen activators and plasminogen activator inhibitor 1 in dedifferentiated chondrosarcoma. *Cancer* **1997**, *79*, 53–58.

- (26) Ammar, H.; Closset, J. L. Clusterin activates survival through the phosphatidylinositol 3-kinase/Akt pathway. *J. Biol. Chem.* **2008**, *283*, 12851–12861.
- (27) Wu, C. C.; Chien, K. Y.; Tsang, N. M.; Chang, K. P.; Hao, S. P.; Tsao, C. H.; Chang, Y. S.; Yu, J. S. Cancer cell-secreted proteomes as a basis for searching potential tumor markers: nasopharyngeal carcinoma as a model. *Proteomics* **2005**, *5*, 3173–3182.
- (28) Chauhan, S. S.; Goldstein, L. J.; Gottesman, M. M. Expression of cathepsin L in human tumors. *Cancer Res.* **1991**, *51*, 1478–1481.
- (29) Ross, P. L.; Cheng, I.; Liu, X.; Cicek, M. S.; Carroll, P. R.; Casey, G.; Witte, J. S. Carboxypeptidase 4 gene variants and early-onset intermediate-to-high risk prostate cancer. *BMC Cancer* **2009**, *9*, 69.
- (30) Said, N.; Frierson, H. F., Jr.; Chernauskas, D.; Conaway, M.; Motamed, K.; Theodorescu, D. The role of SPARC in the tramp model of prostate carcinogenesis and progression. *Oncogene* **2009**, *28*, 3487–3498.
- (31) Arnold, S. A.; Brekken, R. A. SPARC: a matricellular regulator of tumorigenesis. *J. Cell Commun. Signal.* **2009**, *3*, 255–273.
- (32) Clark, C. J.; Sage, E. H. A prototypic matricellular protein in the tumor microenvironment—where there's SPARC, there's fire. *J. Cell Biochem.* **2008**, *104*, 721–732.
- (33) Sage, E. H.; Bassuk, J. A.; Yost, J. C.; Folkman, M. J.; Lane, T. F. Inhibition of endothelial cell proliferation by SPARC is mediated through a Ca(2+)-binding EF-hand sequence. *J. Cell Biochem.* **1995**, *57*, 127–140.
- (34) Goldblum, S. E.; Ding, X.; Funk, S. E.; Sage, E. H. SPARC (secreted protein acidic and rich in cysteine) regulates endothelial cell shape and barrier function. *Proc. Natl. Acad. Sci. U.S.A.* **1994**, *91*, 3448–3452.
- (35) Shankavaram, U. T.; DeWitt, D. L.; Funk, S. E.; Sage, E. H.; Wahl, L. M. Regulation of human monocyte matrix metalloproteinases by SPARC. *J. Cell Physiol.* **1997**, *173*, 327–334.
- (36) Gilles, C.; Bassuk, J. A.; Pulyaeva, H.; Sage, E. H.; Foidart, J. M.; Thompson, E. W. SPARC/osteonectin induces matrix metalloproteinase 2 activation in human breast cancer cell lines. *Cancer Res.* **1998**, *58*, 5529–5536.
- (37) Podgorski, I.; Linebaugh, B. E.; Koblinski, J. E.; Rudy, D. L.; Herroon, M. K.; Olive, M. B.; Sloane, B. F. Bone marrow-derived cathepsin K cleaves SPARC in bone metastasis. *Am. J. Pathol.* **2009**, *175*, 1255–1269.
- (38) Bradshaw, A. D.; Sage, E. H. SPARC, a matricellular protein that functions in cellular differentiation and tissue response to injury. *J. Clin. Invest.* **2001**, *107*, 1049–1054.
- (39) Diaz, V. M.; Hurtado, M.; Thomson, T. M.; Reventos, J.; Paciucci, R. Specific interaction of tissue-type plasminogen activator (t-PA) with annexin II on the membrane of pancreatic cancer cells activates plasminogen and promotes invasion in vitro. *Gut* **2004**, *53*, 993–1000.
- (40) Pallares, I.; Bonet, R.; Garcia-Castellanos, R.; Ventura, S.; Aviles, F. X.; Vendrell, J.; Gomis-Ruth, F. X. Structure of human carboxypeptidase A4 with its endogenous protein inhibitor, latexin. *Proc. Natl. Acad. Sci. U.S.A.* **2005**, *102*, 3978–3983.
- (41) Svatek, R. S.; Karam, J.; Karakiewicz, P. I.; Gallina, A.; Casella, R.; Roehrborn, C. G.; Shariat, S. F. Role of urinary cathepsin B and L in the detection of bladder urothelial cell carcinoma. *J. Urol.* **2008**, *179*, 478–484.
- (42) Staack, A.; Tolic, D.; Kristiansen, G.; Schnorr, D.; Loening, S. A.; Jung, K. Expression of cathepsins B, H, and L and their inhibitors as markers of transitional cell carcinoma of the bladder. *Urology* **2004**, *63*, 1089–1094.
- (43) Staack, A.; Koenig, F.; Daniltchenko, D.; Hauptmann, S.; Loening, S. A.; Schnorr, D.; Jung, K.; Cathepsins, B, H, L activities in urine of patients with transitional cell carcinoma of the bladder. *Urology* **2002**, *59*, 308–312.
- (44) Span, P. N.; Witjes, J. A.; Grebenchtchikov, N.; Geurts-Moespot, A.; Moonen, P. M.; Aalders, T. W.; Vriesema, J. L.; Kiemeneij, L. A.; Schalken, J. A.; Sweep, F. C. Components of the plasminogen activator system and their complexes in renal cell and bladder cancer: comparison between normal and matched cancerous tissues. *BJU Int.* **2008**, *102*, 177–182.
- (45) Sosa, M. S.; Girotti, M. R.; Salvatierra, E.; Prada, F.; de Olmo, J. A.; Gallango, S. J.; Albar, J. P.; Podhajcer, O. L.; Llera, A. S. Proteomic analysis identified N-cadherin, clusterin, and HSP27 as mediators of SPARC (secreted protein, acidic and rich in cysteines) activity in melanoma cells. *Proteomics* **2007**, *7*, 4123–4134.
- (46) Orenes-Pinero, E.; Barderas, R.; Rico, D.; Casal, J. I.; Gonzalez-Pisano, D.; Navajo, J.; Algaba, F.; Piulats, J. M.; Sanchez-Carbayo, M. Serum and tissue profiling in bladder cancer combining protein and tissue arrays. *J. Proteome Res.* **2010**, *9*, 164–173.
- (47) Grassadonia, A.; Tinari, N.; Iurisci, I.; Piccolo, E.; Cumashi, A.; Innominato, P.; D'Egidio, M.; Natoli, C.; Piantelli, M.; Iacobelli, S. 90K (Mac-2 BP) and galectins in tumor progression and metastasis. *Glycoconj. J.* **2004**, *19*, 551–556.
- (48) Yamanaka, M.; Kanda, K.; Li, N. C.; Fukumori, T.; Oka, N.; Kanayama, H. O.; Kagawa, S. Analysis of the gene expression of SPARC and its prognostic value for bladder cancer. *J. Urol.* **2001**, *166*, 2495–2499.
- (49) Tu, C.; Ortega-Cava, C. F.; Chen, G.; Fernandes, N. D.; Cavallo-Medved, D.; Sloane, B. F.; Band, V.; Band, H. Lysosomal cathepsin B participates in the podosome-mediated extracellular matrix degradation and invasion via secreted lysosomes in v-Src fibroblasts. *Cancer Res.* **2008**, *68*, 9147–9156.

PR100189D